Accepted to J. Chem. Phys. 10.1063/5.0137096

ACCEPTED MANUSCRIPT

The Journal of Chemical Physics

AIP Publishing

This is the author's peer reviewed, accepted manuscript. However, the online version of record will be different from this version once it has been copyedited and typeset.
PLEASE CITE THIS ARTICLE AS DOI: 10.1063/5.0137096

A study of core-excited states of organic molecules computed with the generalized active space driven similarity renormalization group

Meng Huang and Francesco A. Evangelista[a)]

Department of Chemistry and Cherry Emerson Center for Scientific Computation, Emory University, Atlanta, Georgia, 30322, U.S.A.

(Dated: 2 March 2023)

This work examines the accuracy and precision of X-ray absorption spectra computed with a multireference approach that combines generalized active space (GAS) references with the driven similarity renormalization group (DSRG). We employ the X-ray absorption benchmark of organic molecules (XABOOM) set, consisting of 116 transitions from mostly organic molecules [T. Fransson *et al.*, *J. Chem. Theory Comput.* **17**, 1618 (2021)]. Several approximations to a full-valence active space are examined and benchmarked. Absolute excitation energies and intensities computed with the GAS-DSRG truncated to second-order in perturbation theory are found to systematically underestimate experimental and reference theoretical values. Third-order perturbative corrections significantly improve the accuracy of GAS-DSRG absolute excitation energies, bringing the mean absolute deviation from experimental values down to 0.32 eV. The ozone molecule and glyoxylic acid are particularly challenging for second-order perturbation theory and are examined in detail to assess the importance of active space truncation and intruder states.

[a)]Electronic mail: francesco.evangelista@emory.edu

Accepted to J. Chem. Phys. 10.1063/5.0137096

ACCEPTED MANUSCRIPT

The Journal of Chemical Physics

AIP Publishing

This is the author's peer reviewed, accepted manuscript. However, the online version of record will be different from this version once it has been copyedited and typeset.
PLEASE CITE THIS ARTICLE AS DOI: 10.1063/5.0137096

I. INTRODUCTION

X-ray absorption spectroscopy (XAS) is a valuable technique for probing the electronic and nuclear structure of molecules as it provides complementary information to other spectroscopies.[1,2] In XAS experiments, absorption of a photon excites a core electron to a valence or continuum orbital, providing information about unoccupied states and the local geometric structure. The development in very recent years of X-ray transient absorption spectroscopy (XTAS)[3–5] has allowed the high-resolution, time-resolved detection of molecules during chemical reactions. This new technique has been applied to investigate various processes, including bond dissociation[6,7], ring-opening reactions[8], intersystem crossing[9,10] and non-adiabatic dynamics.[11–14]

The rapid development of X-ray spectroscopies has increased the need for accurate and efficient electronic structure theories.[15,16] Many computational approaches have been developed for predicting core-excited state. Methods based on density functional theory[17–36] are widely used in the simulation of core excited states due to their low computational cost. On the other hand, systematically improvable (and generally more expensive) wave function methods have been proposed.[10,37–65] The majority of these methods are based on a single-reference formalism and often express core-excited states starting from the ground state wave function. As a consequence, when the initial state is not well described by a single electron configuration (e.g., a molecule far from its equilibrium geometry), errors in the wave function propagate to the excited states resulting in a poor description of potential energy surfaces. To overcome the limitations of single-reference approaches, many multi-reference (MR) methods have been developed for treating core-excited states, including multiconfigurational self-consistent-field (MCSCF) approaches,[66–69] multi-reference algebraic diagrammatic construction,[70] MR configuration interaction,[71–73] and multireference coupled cluster theories.[74–77]

We recently developed a state-specific multi-reference approach to compute core-excited states using general active space self-consistent field (GASSCF) reference wave functions and treating dynamical correlation effects with the driven similarity renormalization group (DSRG).[78] By simulating the vibrationally-resolved XAS of diatomic molecules using a full-valence active space, we have shown that this method can accurately describe core-excited states in the bond-dissociation region, even for systems like CO^+ and N_2^+ that display significant spin coupling effects. Our work also showed the importance of treating dynamical electron correlation beyond second order in perturbation theory, considering third-order and nonperturbative truncation schemes that include

Accepted to J. Chem. Phys. 10.1063/5.0137096

ACCEPTED MANUSCRIPT

The Journal of Chemical Physics

AIP Publishing

This is the author's peer reviewed, accepted manuscript. However, the online version of record will be different from this version once it has been copyedited and typeset.
PLEASE CITE THIS ARTICLE AS DOI: 10.1063/5.0137096

single and double substitutions. In this work, we examine various ways to extend the applicability of the GASSCF-based DSRG approach to medium-sized molecules and to evaluate transition intensities. Firstly, due to limitations on the size of the GAS that can be treated efficiently, we investigate how to extend computations to large molecules by approximating the full-valence active space. Secondly, we employ a state-averaged (SA) extension of MR-DSRG theory[79] to evaluate intensities and deal with problematic conjugated organic systems, where both core and delocalized π orbitals may be near degenerate and can cause root flipping problems. To test the performance of this MR-DSRG approach we use the XABOOM set, an XAS benchmark set containing 40 organic molecules.[80]

The article is structured as follows. In Sec. II we briefly summarize the GAS and state-averaged MR-DSRG approaches. In Sec. III we provide details of the computations performed in this study, including the approximations we applied for larger systems and the choice of the DSRG flow parameter used. In Sec. IV we compare vertical transition energies and relative splittings computed with GAS-DSRG against those from the frozen-core core-valence-separated equation-of-motion coupled cluster theory with singles and doubles (fc-CVS-EOM-CCSD)[51,81] and experiment. We also discuss several systems for which MR-DSRG predictions deviate significantly from the fc-CVS-EOM-CCSD ones. In Sec. V we summarize our results and provide a perspective for future applications of MR-DSRG theory to XTAS simulations.

II. THEORY

This section summarizes the Generalized Active Space Multi-Reference Driven Similarity Renormalization Group (GAS-DSRG) theory we introduced in our previous study on core-excited states of diatomic molecules.[78] The combination of state-averaged GASSCF and DSRG theory allows us to account for static and dynamical electron correlation in the ground and core-excited states. We will focus on the main features of the state-averaged scheme and the evaluation of intensities, two new aspects introduced in this study. The details of the state-averaged implementation of DSRG can be found in Ref. 79. An outline of the state-averaged GAS-DSRG computational scheme is shown in Fig. 1. Compared to the state-specific scheme, which targets one state at the time, the state-averaged formalism can obtain a manifold of solutions in one computation, avoiding root flipping problems.

Accepted to J. Chem. Phys. 10.1063/5.0137096

ACCEPTED MANUSCRIPT

The Journal of Chemical Physics

AIP Publishing

This is the author's peer reviewed, accepted manuscript. However, the online version of record will be different from this version once it has been copyedited and typeset.
PLEASE CITE THIS ARTICLE AS DOI: 10.1063/5.0137096

A. State-averaged GASSCF reference states

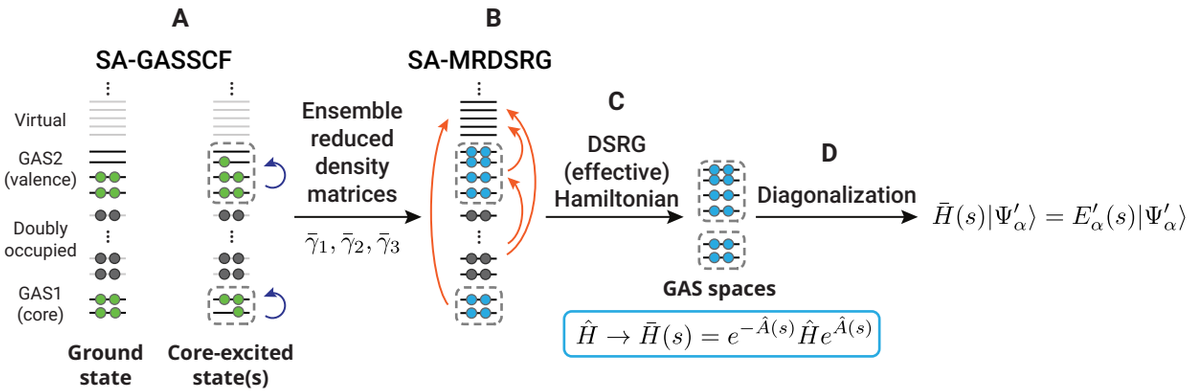

FIG. 1. Computational scheme employed to predict core-excited states using state-averaged GASSCF references and the state-averaged multireference DSRG approach. (A) The ground and target core-excited states are approximated to zeroth-order with several state-averaged GASSCF references (obtained by imposing different GAS constraints). (B) Dynamical correlation effects are optimized for each separate ensemble of states (a group of GASSCF solution with the same occupation restrictions) using a truncated MR-DSRG method. This step requires the 1-,2-, and 3-body ensemble-averaged reduced density matrices of the GASSCF reference. (C) The converged DSRG amplitudes are used to build the DSRG effective Hamiltonian ($\bar{H}$). (D) Diagonalization of $\bar{H}$ provides the relaxed energies E'_α and references Ψ'_α.

We first model the core-excited states using a set of state-averaged GASSCF zeroth-order reference states $\Psi_\alpha, \alpha = 1, 2, ..., m$ which account for static correlation in the core and valence orbitals (with all states built from a unique set of orbitals). Each reference state is a generalized active space self-consistent-field wave function of the form

$$|\Psi_\alpha\rangle = \sum_{\mu}^{\text{GAS}} C_\alpha^\mu |\Phi_\mu\rangle, \tag{1}$$

where $|\Phi_\mu\rangle$ is a determinant that satisfies the GAS restrictions and C_α^μ is the corresponding coefficient. The GAS approach partitions the orbitals into the core, active, and virtual orbitals as in CAS, but further splits the active space into multiple subspaces (GASn, with $n = 1, 2, \ldots$). By imposing restrictions on the maximum/minimum number of electrons occupying each GASn space, specific electronic states can be targeted. For core-excited states, the GAS1 space comprises the core orbitals from which electrons are removed, and the GAS2 spaces includes selected occupied

Accepted to J. Chem. Phys. 10.1063/5.0137096

ACCEPTED MANUSCRIPT

The Journal of Chemical Physics

AIP Publishing

This is the author's peer reviewed, accepted manuscript. However, the online version of record will be different from this version once it has been copyedited and typeset.
PLEASE CITE THIS ARTICLE AS DOI: 10.1063/5.0137096

and unoccupied valence orbitals. Note that we describe different electronic states with different groups of GASSCF solutions (herein referred to as ensembles). For example, the ground electronic state is described by a GAS reference, restricting the GAS1 to be fully occupied. Other GAS subspaces can be introduced to include the effect of semi-core levels, an extension not explored in this work. In these GASSCF computations, orbital rotations between two different GAS are frozen to prevent the collapse of a core-excited state to the ground state, a widely used approximation in core-excited state calculations.[68,82–84] Furthermore, we freeze the number of electrons within each GAS in both the ground and excited state calculations. An alternative approach used in this work is to employ one set of reference GASSCF orbitals for both the ground and core-excited states. In our experience, we found that the resulting orbitals are inadequate to describe states with such different electronic structures. The resulting transition energies typically show absolute errors of the order of 2 eV or more and, therefore, are too inaccurate for simulating XAS.

B. State-averaged multi-reference DSRG theory

After generating the GASSCF reference states, we include the missing dynamical electron correlation via the state-averaged multi-reference DSRG.[79] To this end, for each ensemble of states we build an effective Hamiltonian ($\bar{H}$), which is later diagonalized in the space of ensemble GAS determinants. This state-averaged formalism starts by considering an ensemble of GASCI states ($\{\Psi_\alpha\}$) described by the density operator ($\hat{\rho}$):

$$\hat{\rho} = \sum_{\alpha=1}^{m} \omega_\alpha |\Psi_\alpha\rangle\langle\Psi_\alpha|, \tag{2}$$

where m is the number of states, ω_α is the weight of each state, and $\sum_{\alpha=1}^{m} \omega_\alpha = 1$.

In the state-averaged version of DSRG theory, we build an effective Hamiltonian via the following unitary transformation

$$\hat{H} \to \bar{H} = e^{-\hat{A}} \hat{H} e^{\hat{A}}, \tag{3}$$

where the operator $\hat{A} = \hat{T} - \hat{T}^\dagger$ is anti-Hermitian and expressed in terms of a generalized form of the coupled cluster excitation operator $\hat{T}$. In the state-averaged DSRG, the goal of this unitary transformation is to fold dynamic correlation effects into $\bar{H}$ and achieve a partial decoupling of the ensemble density matrix from the components that involve excited configurations. These components of $\bar{H}$ are referred to as non-diagonal, and are indicated with $\bar{H}^N$. When this decoupling is achieved exactly [i.e., $\bar{H}^N = 0$], one can obtain the eigenvalues for a manifold of states by diagonalizing $\bar{H}$ in the space of GAS determinants that enter into each ensemble. To obtain $\bar{H}$ we

Accepted to J. Chem. Phys. 10.1063/5.0137096

ACCEPTED MANUSCRIPT

The Journal of Chemical Physics

AIP Publishing

This is the author's peer reviewed, accepted manuscript. However, the online version of record will be different from this version once it has been copyedited and typeset.
PLEASE CITE THIS ARTICLE AS DOI: 10.1063/5.0137096

employ a form of operator normal ordering in which expectation values computed with respect to the density matrix $\hat{\rho}$ are zero.[85,86]

To avoid numerical instabilities in solving for the condition, $\bar{H}^N = 0$, caused by small denominators (related to the intruder state problem), the DSRG amplitudes are obtained by solving the following set of many-body equations,

$$\bar{H}^N(s) = \hat{R}(s), \tag{4}$$

where the off-diagonal term $\bar{H}^N(s)$ is gradually driven to zero by *source* operator, $\hat{R}(s)$, in such a way that when $s \to \infty$ we recover the condition $\bar{H}^N = 0$. The source operator that enters in Eq. (4) depends on the number s, referred to as the *flow parameter*. This quantity controls the magnitude of the amplitude that enter into the operator $\hat{A}$, and its presence imparts an s-dependence onto all quantities that enter into $\bar{H}$, including the amplitudes in $\hat{A}$. The choice of the flow parameter using in the GAS-DSRG computations is discussed in Sec. III B. For the full definition of the source operator and the state-averaged DSRG equations, we refer the reader to Ref. 79. The only modification applied compared to the original state-averaged formalism is setting to zero amplitudes that correspond to excitations between different GAS spaces. v

Once the DSRG amplitudes are obtained, the state-averaged DSRG energy is computed by diagonalizing $\bar{H}(s)$ in the space of GAS determinants

$$\bar{H}(s)\,|\Psi'_\alpha\rangle = E'_\alpha(s)\,|\Psi'_\alpha\rangle\,, \tag{5}$$

where E'_α and $|\Psi'_\alpha\rangle$, with $\alpha = 1, \ldots, m$, are *relaxed* energies and references, respectively.

In this work, we focus mainly on perturbative approximations of the MR-DSRG[4,87] for core-excited states. The zeroth-order Hamiltonian is the diagonal component of the generalized Fock matrix, and we work in a semi-canonical basis so this operator is diagonal in the core, valence, and individual GAS spaces. Truncation of the MR-DSRG using this partitioning leads to second and third-order DSRG multi-reference perturbation theories (DSRG-MRPTn, $n = 2, 3$).[4,87] The availability of efficient implementations of these DSRG perturbative methods[88] (and that require at most the three-body reduced density matrices of the GAS references) allows us to easily perform DSRG-MRPT2/3 calculations of multiple core-excited states of relatively large molecules such as DNA nucleobases. For the calculations on ozone, we also consider a nonperturbative approximation to the DSRG termed LDSRG(2), which truncates $\hat{A}$ to one- and two-body substitution operators.[89] Like the parent MR-DSRG theory based on CASSCF references, the GAS-DSRG approach is size

Accepted to J. Chem. Phys. 10.1063/5.0137096

ACCEPTED MANUSCRIPT

The Journal of Chemical Physics

AIP Publishing

This is the author's peer reviewed, accepted manuscript. However, the online version of record will be different from this version once it has been copyedited and typeset.
PLEASE CITE THIS ARTICLE AS DOI: 10.1063/5.0137096

consistent and size extensive, with the former condition being satisfied if the GAS reference is multiplicatively separable. The GAS-DSRG excitation energies are also size intensive, i.e., the transition energies of a supermolecular system composed of noninteracting fragments are identical to those of the isolated fragments. We verified the size intensivity of GAS-DSRG at second order in perturbation theory by considering the lowest O K-edge transition in CO. The energy and intensity of a supermolecular system containing CO and a Ne atom at a finite distance were found to be different from those of isolated CO, but converge to those for an isolated CO as the distance between these fragments goes to infinity.

C. Evaluation of oscillator strengths

In this study, we also extend our approach to evaluate the transition oscillator strength between ground and core-excited states. We approximate the transition oscillator strength using the relaxed GAS states, where the ground state wave function employs orbitals optimized for core-excited states. This approximation captures the bulk of the transition oscillator strength but neglects orbital relaxation effects in the ground state and contributions from dynamical correlation. In practice, for each ensemble of states, we perform a state-averaged GASSCF computation in which, in addition to the m target core-excited states, we include a state with fully occupied GAS1(core) and zero weight ($\omega_0 = 0$). We then approximate the transition dipole moment between the ground state ($\alpha = 0$) and core-excited state α ($d_{0\alpha}$) as

$$d_{0\alpha} = \sum_{pq} \mu_{pq} \langle \Psi_0 | \hat{a}_q^p | \Psi_\alpha \rangle, \tag{6}$$

where $\vec{\mu}_{pq} = \langle \phi_p | \vec{\mu} | \phi_q \rangle$ is the molecular orbital dipole moment matrix and $\langle \Psi_\alpha | \hat{a}_q^p | \Psi_\beta \rangle$ is the transition one-body reduce density matrix. Note that transition energies are instead computed using a fully optimized ground state GAS reference.

III. COMPUTATIONAL DETAILS

To benchmark the accuracy of GAS-DSRG theories on core-excited states, we employ the XABOOM benchmark set,[80] which contains 1s $\rightarrow \pi^*$ transitions for a total of 40 molecules of different size. We use molecular geometries optimized at the frozen-core MP2/cc-pVTZ level of theory (taken from Ref. 80). Vertical transition energies computed with GAS-DSRG are computed according to a procedure similar to our previous study.[78] First, ground-state molecular orbitals are obtained using restricted Hartree-Fock (RHF) and the cc-pVQZ basis.[90] These orbitals are

Accepted to J. Chem. Phys. 10.1063/5.0137096

ACCEPTED MANUSCRIPT

The Journal of Chemical Physics

AIP Publishing

This is the author's peer reviewed, accepted manuscript. However, the online version of record will be different from this version once it has been copyedited and typeset.
PLEASE CITE THIS ARTICLE AS DOI: 10.1063/5.0137096

then separately optimized using state-averaged GASSCF for the ground and core-excited electronic states.

A. Approximations

For larger systems, it is necessary to introduce approximations to reduce the time and memory cost of the GAS-DSRG calculations. To reduce storage costs, density fitting of the two-electron integrals was applied on molecules with more than five atoms, using the cc-pVQZ-JKFIT[91] and cc-pVQZ-RIFIT[92] auxiliary basis sets for state-averaged GASSCF and MR-DSRG, respectively. Furthermore, we did not account for relativistic effects. Following the XABOOM study,[80] we also used the cc-pVQZ basis which lacks the flexibility to treat core-valence correlation.

As in our previous treatment,[78] the core orbitals pertinent to a target transition are included in the GAS1, while the active valence orbitals are all in the GAS2. To denote the choice of active space and the constraints on the number of electrons, a GAS occupation is denoted by $(n_{\mathrm{o}}^1\mathrm{o}, n_{\mathrm{e}}^1\mathrm{e}; n_{\mathrm{o}}^2\mathrm{o}, n_{\mathrm{e}}^2\mathrm{e}; \cdots)$, where n_{o}^m and n_{e}^m are the number of orbitals and electrons in the m-th GAS space, respectively. For molecules with two heavy (non-hydrogen) atoms, the GAS2 space spans the full valence orbitals ($2s$+$2p$). For molecules with three heavy atoms, only the $2p$ orbitals of the heavy atoms are included in GAS2, except for the highly symmetric O_3 and N_2O molecules for which full valence orbitals are used. For systems with four or more heavy atoms, the GAS1 consists of the 1s core orbitals of the heavy atoms and the GAS2 consists of $(2p)\pi$ orbitals. The selection of the π orbitals is straightforward for molecules with C_s or higher symmetry. However, for systems with C_1 symmetry, especially the nucleobases with pseudo-planar equilibrium geometries, the π orbitals must be manually selected. For C_4F_6 in the benchmark set (C_1 symmetry), the GAS2 space contains only 6 orbitals around the LUMO/HOMO levels.

Most of the GAS-DSRG calculations are performed averaging over several electronic states. This is mainly to avoid variational collapse in the GASSCF optimization due to the small energy gap between core-excited states. Moreover, it is crucial to ensure a consistent determinantal composition of the electronic state(s) before and after diagonalization of the DSRG effective Hamiltonian. By default, all the $N_c \times N_\pi$ singly excited states, where N_c is the number of cores and N_π is the number of low energy unoccupied π orbitals, are averaged. However, for some of the molecules, we observe root flipping after the DSRG perturbative treatment, especially at the DSRG-MRPT2 level, a problem we address by increasing the number of roots averaged. For larger systems with a high density of states (especially for the carbon and nitrogen K-edge calculations of

Accepted to J. Chem. Phys. 10.1063/5.0137096

ACCEPTED MANUSCRIPT

The Journal of Chemical Physics

AIP Publishing

This is the author's peer reviewed, accepted manuscript. However, the online version of record will be different from this version once it has been copyedited and typeset.
PLEASE CITE THIS ARTICLE AS DOI: 10.1063/5.0137096

nucleobases), we perform separate computations on atoms with different chemical environments (split-core method), whereby the GAS1 only consists of one core orbital for each calculation. The active spaces and states averaged for all GAS-DSRG calculations are listed in Table S1 of the Supplementary Material.

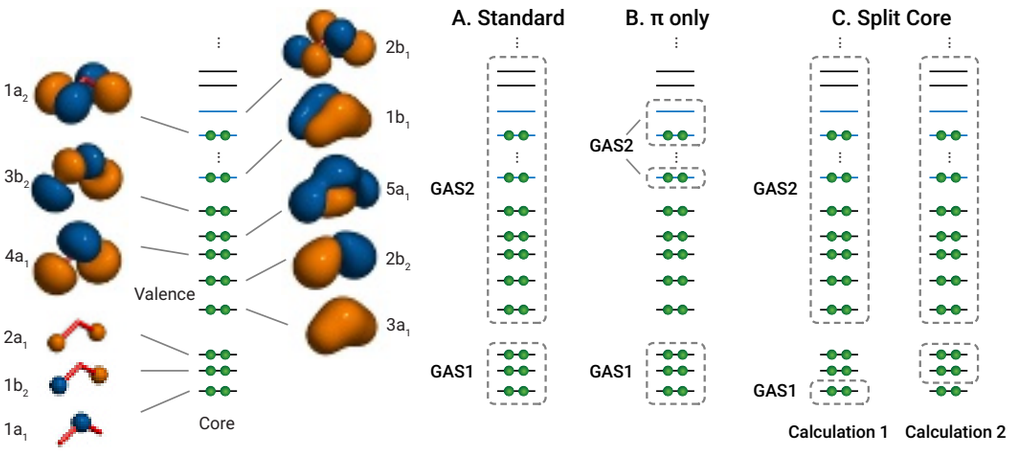

FIG. 2. Definition of the GAS1 and GAS2 orbital spaces for the ozone GAS-DSRG calculation. (A) Standard full valence space. (B) GAS partitioning used for the π only approximation. (C) GAS partitioning used in the split core approximation (two separate calculations).

To assess the impact of these approximations and the choice of the active space, we ran benchmark computations on two systems, N_2O and O_3. The active space tested for O_3 are shown in Fig. 2. The "standard" choice of active space includes all the 1s core orbital in GAS1 and all the valence orbitals in GAS2, leading to a (3o, 5e; 12o, 19e) GAS. The "π only" (PO) treatment includes only π orbitals in the GAS2 space, reducing the GAS to the much smaller (3o, 5e; 3o, 5e). In both cases, a total of 8 states are averaged. The "Split Core"(SC) strategy performs two different state-averaged calculations; the first one focuses on the central oxygen core excitations, and uses the GAS (1o, 1e; 12o, 19e), averaging two states. The second one considers core excitations from the terminal oxygens, and uses the GAS (2o, 3e; 12o, 19e), averaging over 6 states. We can also apply the PO and SC approximation together (PO+SC). Similar approximations are considered on the N K-edge calculation of N_2O in which "standard" choice of active space is (2o, 3e; 12o, 17e). The transition energies and oscillator strengths of excitations from the 1s core orbital of the central atom (denoted by the subscript C) and the terminal atom (denoted by the subscript T) computed with different active spaces are reported in Table I. We also reported the energy difference, $\Delta E = E_C - E_T$, and the ratio of oscillator strengths, f_T/f_C between the two transitions,

Accepted to J. Chem. Phys. 10.1063/5.0137096

ACCEPTED MANUSCRIPT

The Journal of Chemical Physics

AIP Publishing

This is the author's peer reviewed, accepted manuscript. However, the online version of record will be different from this version once it has been copyedited and typeset.
PLEASE CITE THIS ARTICLE AS DOI: 10.1063/5.0137096

TABLE I. K-edge transition energies (E, in eV) and oscillator strengths (f) for the terminal (T) and central (C) O/N atoms in O_3/N_2O computed with the GAS-DSRG using different truncation schemes and choices of GAS. Energy differences between two transitions (ΔE, in eV) are also reported. Results were computed with a GASSCF reference and different levels of theory [PT2 = DSRG-MRPT2, PT3 = DSRG-MRPT3] using the cc-pVQZ basis. The numbers in parenthesis show differences with respect to "standard" values.

Molecule	Method	Approximations	E_T	f_T	E_C	f_C	ΔE	f_T/f_C
O_3	PT2	Standard	527.95	0.0817	533.12	0.0322	5.16	0.39
		PO	522.59	0.0810	528.70	0.0376	6.11 (+0.95)	0.46
		SC	527.99	0.0886	534.31	0.0504	6.32 (+1.16)	0.57
		SC + PO	525.79	0.0727	535.09	0.0953	9.30 (+4.14)	1.31
	PT3	Standard	530.24	0.0773	535.38	0.0326	5.14	0.42
		PO	532.34	0.0792	537.74	0.0387	5.40 (+0.26)	0.49
		SC	529.81	0.0854	534.67	0.0491	4.86 (−0.28)	0.58
		SC + PO	530.25	0.0953	535.11	0.0682	4.85 (−0.29)	0.72
N_2O	PT2	Standard	400.47	0.0505	403.97	0.0544	3.50	1.08
		PO	399.74	0.0529	403.25	0.0594	3.51 (+0.01)	1.12
		SC	400.51	0.0562	404.26	0.0616	3.75 (+0.25)	1.10
		SC + PO	400.22	0.0531	403.87	0.0565	3.65 (+0.15)	1.06
	PT3	Standard	401.20	0.0502	404.72	0.0556	3.53	1.11
		PO	401.37	0.0515	404.81	0.0587	3.45 (−0.08)	1.14
		SC	400.77	0.0563	404.52	0.0620	3.75 (+0.22)	1.10
		SC + PO	400.80	0.0574	404.48	0.0626	3.67 (+0.14)	1.09

which are perhaps better criteria for measuring the accuracy of core-excited state calculations.

Several observations can be made from this initial test. First, the effect of partitioning and excluding orbitals from the active space is much more substantial in O_3 compared to N_2O. Under all approximations, ΔE values for N_2O deviate less than 0.3 eV from the "standard" results. For O_3, at DSRG-MRPT2 level, the deviation from the "standard" results are already about 1 eV from both the PO and SC approximations, increasing significantly (to 4.14 eV) when PO and SC are combined. A similar observation can also be made for the oscillator strength ratio. This significant difference

Accepted to J. Chem. Phys. 10.1063/5.0137096

ACCEPTED MANUSCRIPT

The Journal of Chemical Physics

AIP Publishing

This is the author's peer reviewed, accepted manuscript. However, the online version of record will be different from this version once it has been copyedited and typeset.
PLEASE CITE THIS ARTICLE AS DOI: 10.1063/5.0137096

is most likely due to the orbital near-degeneracies in the O_3 molecule, which will be discussed in Section IV C 1. Our second observation is that the deviations of ΔE from the standard calculation at the DSRG-MRPT3 level are less than 0.40 eV for all approximations, an error significantly smaller than the aforementioned deviation in DSRG-MRPT2. In addition, compared to the PO approximation, the SC approximation has a stronger impact on the energy splitting between two core-excited states, though the number of determinants in the SC approximation is generally much closer to the standard one.

B. Choice of the flow parameter

We tested the sensitivity of transition energy and dipole moment on the DSRG flow parameter, s, for molecules with different sizes. For valence excitations, a recent benchmark study by Wang, Fang, and Li[93] of 280 transitions showed that the optimal choice of flow parameter is 0.35/2 E_h^{-2} for SA-DSRG-MRPT2/3. In this work, three molecules (ethene, benzene, and naphthalene) are selected as representatives for benchmarking the choice of s, as they share the same elements but vary in size. The active space for ethene [(2o, 3e; 12o, 11e)] consists all the valence orbital, while the active spaces for benzene [(6o, 11e; 6o, 7e)] and naphthalene [(10o, 19e; 10o, 11e)] only include core and π orbitals. The computed transition energies and oscillator strength of the C 1s $\rightarrow \pi^*$ transitions are shown in Table II. These were computed with different MR-DSRG treatments of dynamical correlation and flow parameter values in the range 0.25–4 E_h^{-2}.

The dependence of oscillator strength on s is not very significant, but the dependence of the transition energies varies with system size. The transition energies for ethene vary by up to 0.6/0.08 eV for DSRG-MRPT2/3, indicating a more pronounced dependence on s than previously observed for N_2^+ (0.1 eV).[78] The variation in transition energy as a function of s is even larger for benzene(ca. 3.5 eV) and naphthalene (ca. 4 eV for three transitions). On the other hand, the relative splittings of three states of naphthalene are affected less by the s parameter, with the splitting between the highest and lowest transitions ranging from 0.90 eV to 1.35 eV at the DSRG-MRPT2 level and from 0.86 to 0.94 eV at the DSRG-MRPT3 level.

An analysis of this data shows that this strong s-dependence of the transition energies is mainly observed for small values of s (0.125–0.25 E_h^{-2}), when important DSRG amplitudes are suppressed and increases with system size due to extensivity of dynamical correlation. We also note that the absolute energies of the ground and core-excited state show different dependences on s, with the latter requiring larger s values to converge. For example, at the DSRG-MRPT2 level, the difference

Accepted to J. Chem. Phys. 10.1063/5.0137096

ACCEPTED MANUSCRIPT

The Journal of Chemical Physics

AIP Publishing

This is the author's peer reviewed, accepted manuscript. However, the online version of record will be different from this version once it has been copyedited and typeset.
PLEASE CITE THIS ARTICLE AS DOI: 10.1063/5.0137096

between the 1s $\rightarrow \pi^*$ core excited state of benzene computed with $s = 1$ and 0.5 E_h^{-2} is 29.2 mE_h, but the same difference is only 4.3 mE_h for the ground state. In practice, we find that using $s = 1$ E_h^{-2} is a good compromise for the absolute transition energy for all our reported calculations. In benzene and naphthalene, this value leads to a shift of absolute transition energies no more than 0.3/0.1 eV for DSRG-MRPT2/3 calculations compared to $s = 2$ E_h^{-2}.

IV. RESULTS AND DISCUSSION

A. Absolute Transition Energies and Oscillator Strengths

To investigate the accuracy of X-ray absorption transition energies predicted with the GAS-DSRG approach, we first compare the DSRG-MRPT2 and DSRG-MRPT3 result with these from fc-CVS-EOM-CCSD,[51] the most accurate theoretical results in the XABOOM set.[80] We note, however, that works that have compared the performance of EOM-CCSD to higher-order coupled cluster methods,[56] show that triple excitations can shift core excitation energies by more than 1 eV and that quadruple excitations are required to achieve sub-eV accuracy. The fc-CVS-EOM-CCSD method applies the frozen-core and core-valence separation, which provides an efficient and robust method for evaluating core-excited state energies. This method uses coupled cluster amplitudes that exclude core orbitals (fc) and restricts the EOM operator to excitations that involve at least one core orbital (CVS). In comparison, in the current DSRG approach, we also enforce the core-valence separation (since the GASSCF solutions that represent core-excited states enforce occupation restrictions on the core orbitals) while we do not apply the frozen-core approximation, since the core orbitals are treated either as active or restricted, and therefore their occupation is modified by the operator $\hat{A}(s)$. For simplicity, we denote the fc-CVS-EOM-CCSD method as EOM-CCSD in the following.

Table III reports error statistics for the relative energy difference between these theories for each of the C, N and O K-edge excitation energies. As it can be seen, the mean signed deviation (MSD) (PT2−CC/PT3−CC) are all negative and relatively close to the mean absolute deviation (MAD) of each set. Figure 3A shows the distribution of computed transition energies differences with respect to EOM-CCSD excitation energies. For the C K-edge transitions, absolute energies computed with the DSRG-MRPT3 and EOM-CCSD show good agreement. Most of the transitions are less than 0.5 eV apart from each other, and the MAD between the two sets is 0.43 eV. The DSRG-MRPT2 results show a much larger deviation (MAD = 1.32 eV) from EOM-CCSD. On the other hand, the

Accepted to J. Chem. Phys. 10.1063/5.0137096

ACCEPTED MANUSCRIPT

The Journal of Chemical Physics

AIP Publishing

This is the author's peer reviewed, accepted manuscript. However, the online version of record will be different from this version once it has been copyedited and typeset.
PLEASE CITE THIS ARTICLE AS DOI: 10.1063/5.0137096

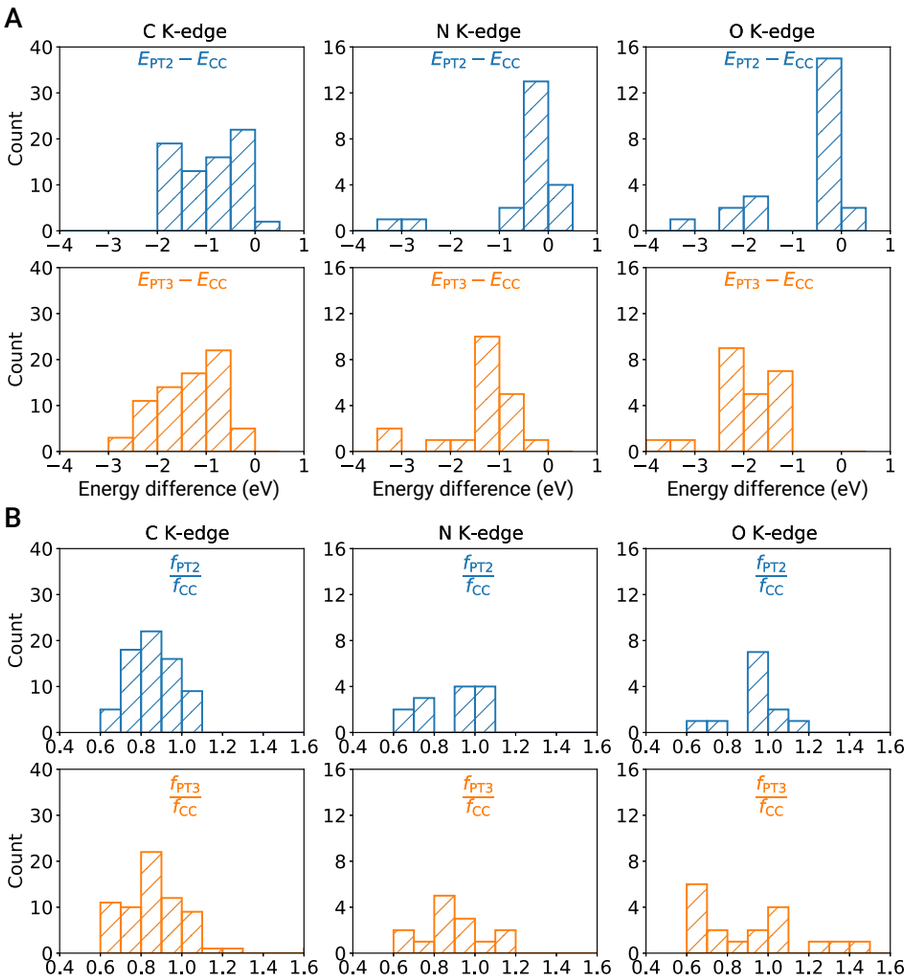

FIG. 3. Comparison of the C, N and O K-edge core-excited states in the XABOOM set computed with the GAS-DSRG and EOM-CCSD. (A) distribution of transition energy differences ($E_{\mathrm{PT}n} - E_{\mathrm{CC}}$) and (B) oscillator strength ratios ($f_{\mathrm{PT}n}/f_{\mathrm{CC}}$) computed for n^{th}-order GAS-DSRG perturbation theory using the cc-pVQZ basis set. EOM-CCSD transition energies (E_{CC}) computed with the same basis set are taken from Ref. 80. The C, N and O K-edge transitions are plotted in different columns.

N K-edge and O K-edge show a somehow different behavior, where the deviation between the two DSRG theories is generally smaller than the deviation from EOM-CCSD. We also computed the oscillator strength for each transitions, and plotted the distribution of the $f_{0\alpha}$ ratios between the three theories in Fig. 3B. The transition oscillator strength ratio between EOM-CCSD and DSRG-MRPT2/3 can vary dramatically, likely due to our approximate way of computing $f_{0\alpha}$ within the state-averaged GAS framework. Computing transition dipole moments using state-averaged GAS

Accepted to J. Chem. Phys. 10.1063/5.0137096

ACCEPTED MANUSCRIPT

The Journal of Chemical Physics

AIP Publishing

This is the author's peer reviewed, accepted manuscript. However, the online version of record will be different from this version once it has been copyedited and typeset.
PLEASE CITE THIS ARTICLE AS DOI: 10.1063/5.0137096

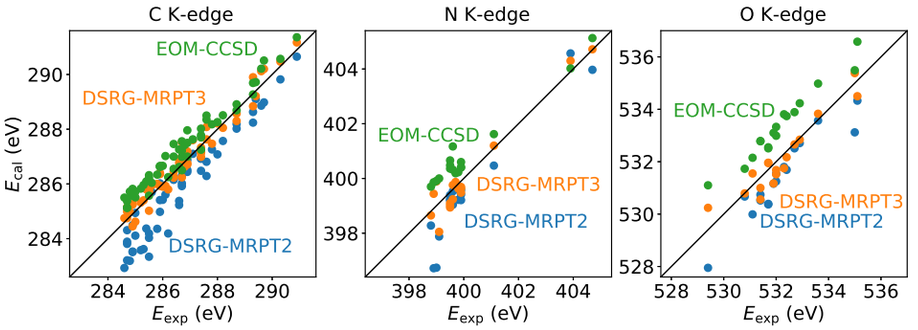

FIG. 4. Comparison between theoretical and experimental the C, N and O K-edge transition energies in the XABOOM set. The DSRG transition energies are computed using DSRG-MRPT2 and DSRG-MRPT3 theories with cc-pVQZ basis. The EOM-CCSD transition energies with the same basis set are from Ref. 80. For each scatter point, the horizontal and vertical axis indicate its experimental and theoretical value, with the diagonal line noting perfect agreement.

with a nonzero weight for the ground state may be a way to improve this approximation. However, preliminary computations show that the agreement with EOM-CCSD results does not improve systematically. Two other potential sources of error in our approximate oscillator strengths come from ignoring dynamical correlation effects and constraining the ground and excited states to use the same orbitals. Improving upon these approximations will be pursued in future research.

The theoretical transition energies are also compared with available experimental values, which are absent from the XABOOM set.[13,94–117] Transition energy distributions are shown in Fig. 4 and error statistics are reported in Table III. The DSRG-MRPT3 results best match the experimental transitions, with the MAD from experiment being only 0.32 eV, a much smaller value than for DSRG-MRPT2 (0.76 eV) and EOM-CCSD (0.70 eV). Moreover, DSRG-MRPT2 (MSE = −0.74 eV) and EOM-CCSD (MSE = 0.70 eV) are more likely to underestimate and overestimate transition energies, respectively. The overestimation of the EOM-CCSD for valence transition energies has been observed previously,[118,119] and Fransson et al.[80] also reported that EOM-CCSD with relativistic corrections overestimates the CO C K-edge, HCN N K-edge, and CO O K-edge by 0.3, 0.7 and 1.2 eV when compared to experiment.

The excellent agreement between DSRG-MRPT3 and experiment may disguise some error cancellation due to the complexity of comparing these X-ray absorption data with experiment, as it has been illustrated in the XABOOM study.[80] Some common assumptions made in the theoretical calculation of X-ray absorption spectra have been assessed in our previous study on diatomic

Accepted to J. Chem. Phys. 10.1063/5.0137096

ACCEPTED MANUSCRIPT

The Journal of Chemical Physics

AIP Publishing

This is the author's peer reviewed, accepted manuscript. However, the online version of record will be different from this version once it has been copyedited and typeset.
PLEASE CITE THIS ARTICLE AS DOI: 10.1063/5.0137096

molecules.[78] For example, the difference between the vertical and the adiabatic transition energy of the CO 1s $\rightarrow \pi^*$ excitation is 0.6 eV from the MR-LDSRG(2) truncation level. Scalar relativistic effects contribute to shifts roughly on the order of 0.2 eV for C, N, and O K-edge transitions, and core-valence correlation basis sets can lead to absolute energy differences as large as 0.5 eV. The existence of all of these uncontrolled factors suggests comparing instead the energy difference between transitions, a topic discussed in the next section.

B. Relative Transition Energies and Intensities

From our results, we computed the energy splittings between transitions for all the molecules for which we compute more than one core-excited state from any type of core atom. For molecules which have more than two transitions, we calculate all the splittings between adjacent transitions. A total of 47 energy splittings are obtained and the error statistics with respect to experimental and theoretical (EOM-CCSD) results are shown in Table IV. Due to the relatively small number of splittings for N/O K-edge transitions, we only report aggregated statistics. For each of these splittings, we also computed the ratio between their transition oscillator strengths. All splittings and oscillator strength ratios are listed in Table S2 of the Supplementary Material.

Compared to the absolute transition energy, the energy splittings listed in the Table IV are less sensitive to different levels of theory. An interesting observation is that in most systems the third-order contribution to the correlation energy has a different sign for ground and core-excited state, explaining the much better agreement in the energy splitting prediction for DSRG-MRPT3 *vs*. DSRG-MRPT2. For the 34 splittings where an experimental value is available, the statistics show no significant difference among theories. This is partly due to the limited resolution of experiments, where some splittings are simply unresolved. As most of systems in the XABOOM set have close-shell ground states, this relative good agreement in the energy splittings is expected. However, there are several systems where large deviations in the energy splittings (>0.40 eV) can still be observed among the theories. We will discuss these systems in the next section.

C. Special cases

1. *Ozone*

Our computations show significant discrepancies between the GAS-DSRG and EOM-CCSD predictions for ozone. The ground state of ozone is composed of two closed-shell electron

Accepted to J. Chem. Phys. 10.1063/5.0137096

ACCEPTED MANUSCRIPT

The Journal of Chemical Physics

AIP Publishing

This is the author's peer reviewed, accepted manuscript. However, the online version of record will be different from this version once it has been copyedited and typeset.
PLEASE CITE THIS ARTICLE AS DOI: 10.1063/5.0137096

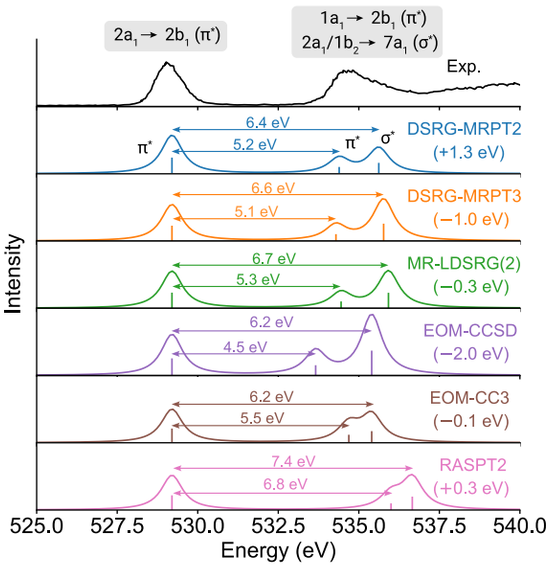

FIG. 5. Experimental and theoretical K-edge X-ray absorption spectra of ozone. The theoretical spectra are computed at the DSRG-MRPT2, DSRG-MRPT3, and MR-LDSRG(2) levels of theory, and convoluted with a Lorentzian of 0.8 eV width. The convoluted spectra from fc-CVS-EOM-CCSD,[51] EOM-CC3,[120] and MS-RASPT2[121] with the same Lorentzian broadening are also plotted. The fc-CVS-EOM-CCSD results are based on a different basis (aug-cc-pVTZ),[122] and the transition energies are affected at most by 0.13 eV compared to the XABOOM ones.[80] The MS-RASPT2 results are based on a smaller activate space (3e, 5o; 9e, 12o) and basis set (cc-pVTZ) compared to our GAS-DSRG calculation. The experimental spectrum is digitized from Ref. 101. Reproduced from *J. Chem. Phys.* **115**, 3614 (2001), with the permission of AIP Publishing.

configurations, the first one corresponding to the occupation $(1a_1)^2(2a_1)^2(1b_2)^2\ldots(6a_1)^2(1a_2)^2$ and the second one corresponding to the doubly excited determinant $(1a_2)^{-2}(2b_1)^2$, where we use a compact notation to express the occupation pattern with respect to the dominant electron configuration. Our GAS-DSRG computations show good agreement for the splittings between the two 1s $\rightarrow \pi^*$ transitions ($2a_1 \rightarrow 2b_1$ and $1a_1 \rightarrow 2b_1$), predicted to be 5.16 and 5.14 eV from DSRG-MRPT2/3 theory. However, the splitting predicted by EOM-CCSD (ca. 4.5 eV) significantly underestimates the experimental value[123] (estimated to be 5.55 eV). This large deviation is likely due to the open-shell character of the ground state of ozone, which has been studied theoretically in the low-lying states,[124–133] core-excited states,[51,121] and core-ionized states.[70,121] To further

Accepted to J. Chem. Phys. 10.1063/5.0137096

ACCEPTED MANUSCRIPT

The Journal of Chemical Physics

AIP Publishing

This is the author's peer reviewed, accepted manuscript. However, the online version of record will be different from this version once it has been copyedited and typeset.
PLEASE CITE THIS ARTICLE AS DOI: 10.1063/5.0137096

analyze this discrepancy, we extended our GAS-DSRG computations to all transitions in the X-ray absorption spectrum of O_3 and compared them with those measured experimentally.[101,123,134] We focus in particular on the more recent works of Rosenqvist *et al.*[101] and Stranges *et al.*,[123] which have addressed deficiencies in earlier measurements.[134] We also applied the MR-LDSRG(2) method, the most accurate nonperturbative truncation scheme available. The active space used in GAS-DSRG calculations is the "standard" active space in Fig. 2.

According to the experimental assignment,[101,123] four core-to-valence transitions in the X-ray absorption region have significant oscillator strength: $1a_1 \rightarrow 2b_1(\pi^*)$, $2a_1 \rightarrow 2b_1(\pi^*)$, $1b_2 \rightarrow 7a_1(\sigma^*)$, and a weak $2a_1 \rightarrow 7a_1(\sigma^*)$ transition which overlaps with the $1b_2 \rightarrow 7a_1(\sigma^*)$ transition. Including these $1s \rightarrow \sigma^*$ transitions requires averaging 16 states. The experimental spectrum and theoretical simulations shifted to match the experiment are shown in Figure 5. For comparison, we have also plotted existing theoretical XAS spectra of ozone from fc-CVS-EOM-CCSD,[51] MS-RASPT2,[121] and EOM-CC3.[120] We note that the work of Stranges *et al.* assigns excitation energies relative to the first line of 5.55 and 6.50 eV.[123] All the GAS-DSRG methods predict a similar triplet feature, with some differences in the relative shifts.

For absolute transition frequencies, it is not surprising to see that the DSRG-MRPT2 requires a large blue shift (+1.3 eV) to match the experiment (a trend discussed in Section IV). However, a large red shift (−1.0 eV) is also necessary for the DSRG-MRPT3, while MR-LDSRG(2) requires only a small shift (−0.3 eV). For all the DSRG simulated spectra, the strong transitions [$1a_1 \rightarrow 2b_1(\pi^*)$ and $1b_2(2a_1) \rightarrow 7a_1(\sigma^*)$] agree well with the experiment. The third $2a_1 \rightarrow 2b_1(\pi^*)$ transition is predicted to be 6.4–6.7 eV above the first line, in agreement with the experimental assignment (6.5 eV);[123] however, the intensity appears to be overestimated, as in the experimental spectrum this peak is not as prominent as in our simulations. There might be several reasons for the observed discrepancy between the GAS-DSRG and experimental spectrum, however, a more detailed investigation of this molecule is beyond the scope of this work. Going beyond EOM-CCSD, the EOM-CC3[120] predictions reproduce well the transition frequencies for all the peaks in the experiment and requires a very small shift (−0.1 eV). Recent MS-RASPT2 results[121] yield a spectrum similar to the EOM-CC3 one; however, the splitting between the two lowest transitions appears to be overestimated (6.8 eV vs. the experimental value 5.55 eV). A GAS-DSRG test calculation using the same active space and basis set used in the MS-RASPT2 study gives transition energies that are within 0.21 eV from our values. Despite the good agreement that can be reached with the excitation energies, none of the theoretical computations satisfactorily reproduce the

Accepted to J. Chem. Phys. 10.1063/5.0137096

ACCEPTED MANUSCRIPT

The Journal of Chemical Physics

AIP Publishing

This is the author's peer reviewed, accepted manuscript. However, the online version of record will be different from this version once it has been copyedited and typeset.
PLEASE CITE THIS ARTICLE AS DOI: 10.1063/5.0137096

intensity profile of the ozone XAS spectrum.

An analysis of the wave function of the core-excited states of ozone validates the need for a multi-reference treatment. Table V lists the leading contributions for the three core-excited states, $2a_1 \rightarrow 2b_1(\pi^*)$, $1a_1 \rightarrow 2b_1(\pi^*)$, and $1b_2 \rightarrow 7a_1(\sigma^*)$ computed at the MR-LDSRG(2) level of theory. The most important contribution to all three core-excited states is due to singly excited configurations with respect to the leading ground state determinant. However, these appear with a weight (54–65 %) smaller than the dominant ground state determinant (ca. 90 %), indicating large configuration mixing in the core-excited states. The second largest contribution to the core-excited states is due to a single excitation out of the $(1a_2)^{-2}(2b_1)^2$ configuration, which appears with a large weight (ca. 16–23 %). The rest of the significant configurations are double excitations (one core-to-valence and one valence-to-valence), and add up to around 20% of the wave function probability. This significant multi-determinantal character of the core-excited states of ozone is consistent with our previous discussion in Section III A where the $1s \rightarrow \pi^*$ transition frequencies showed a strong dependence on the choice of the GAS. All these observations suggest that modeling the core-excited state of ozone requires an accurate treatment of static and dynamical correlations.

2. Glyoxylic Acid

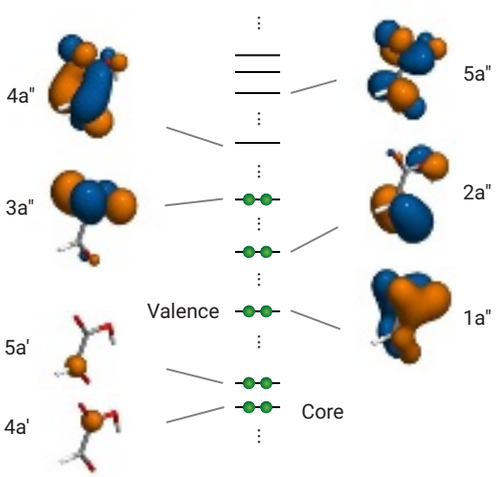

FIG. 6. Molecular orbital included in the active space used to compute the C 1s $\rightarrow \pi^*$ transitions of glyoxylic acid.

Glyoxylic acid (HCOCOOH) is another system where we observe significant discrepancies between different theories. Specifically, of interest are the two $4a' \rightarrow 4a''$ and $5a' \rightarrow 4a''$ carbon

Accepted to J. Chem. Phys. 10.1063/5.0137096

ACCEPTED MANUSCRIPT

The Journal of Chemical Physics

AIP Publishing

This is the author's peer reviewed, accepted manuscript. However, the online version of record will be different from this version once it has been copyedited and typeset.
PLEASE CITE THIS ARTICLE AS DOI: 10.1063/5.0137096

K-edge transitions, denoted by the orbitals involved. These orbitals are plotted in Fig. 6, and the computed frequencies and oscillator strengths of the two transitions are listed in Table VI. Unlike the case of ozone, we observe a significant underestimation of the splitting between transitions at the DSRG-MRPT2 level (1.63 eV for DSRG-MRPT2 vs. ca. 2.10 eV for DSRG-MRPT3 and EOM-CCSD). We also notice underestimation of the $4a' \rightarrow 4a''$ transition oscillator strength by DSRG-MRPT2, as the ratio of the oscillator strengths is 0.51 for DSRG-MRPT2 while 0.95 for DSRG-MRPT3 and 0.92 for EOM-CCSD.

A detailed analysis of the DSRG-MRPT2 wave function shows the $4a' \rightarrow 4a''$ excited state being primarily composed of the $(4a')^{-1}(4a'')^{1}$ configuration (84.1%) plus a small contribution from the $(4a')^{-1}(5a'')^{1}$ configuration (4.3%). However, DSRG-MRPT3 shows a more pronounced multi-determinantal wave function (58.2% and 24.7%), much closer to the composition of the GASSCF reference (38.2% and 36.1%). This is one of several cases where dynamical correlations from second- and third-order perturbation theory give opposite contributions to the determinantal composition of a state, with pyridine and pyridazine being two other examples.

For glyoxylic acid, we have traced this problem to the largest two-body amplitude (0.126), observing that when s is reduced to 0.5 E_h^{-2} its value is reduced to 0.087 and the predicted energy splitting (1.91 eV) and an intensity ratio (0.74) between the two $1s \rightarrow \pi^*$ transitions agree well with DSRG-MRPT3 and EOM-CCSD. The DSRG-MRPT2 wave function is also more multi-determinantal with the $(4a')^{-1}(4a'')^{1}$ and $(4a')^{-1}(5a'')^{1}$ configurations contributing 73.4% and 13.6%, respectively. On the other hand, DSRG-MRPT3 is more robust to changes in s, predicting an energy splitting (2.14 eV) and an intensity ratio (0.98) similar to the corresponding values computed with $s = 1$ E_h^{-2}. The strong dependence on flow parameters indicates that, despite regularization of the small denominators, the DSRG-MRPT2 can show a more pronounced s dependence due to intruders. Interestingly, the split core approximation can also help mitigate the effect of intruder states. In the split core calculations (denoted as SC in Table VI), the largest amplitude ($s = 1$ E_h^{-2}) for the $4a' \rightarrow 4a''$ transition reduces to 0.097 at the DSRG-MRPT2 level of theory. This treatment leads to a 1.72 eV energy splitting and an oscillator strength ratio of 0.60 between the two transitions, closer to the DSRG-MRPT3 ($s = 0.5$ E_h^{-2}) values. A similar trend has also been found for 1,2-benzoquinone, for which the energy splittings and oscillator strength ratio evaluated with $s = 0.5$ and 1 E_h^{-2} are listed in Table S3 of the Supplementary Material.

Accepted to J. Chem. Phys. 10.1063/5.0137096

ACCEPTED MANUSCRIPT

The Journal of Chemical Physics

AIP Publishing

This is the author's peer reviewed, accepted manuscript. However, the online version of record will be different from this version once it has been copyedited and typeset.
PLEASE CITE THIS ARTICLE AS DOI: 10.1063/5.0137096

V. CONCLUSION

This study benchmarks a state-averaged version of the Generalized-Active-Space Driven Similarity Renormalization (GAS-DSRG) approach for computing core-excited electronic states using the XABOOM set.[80] The core-excited states are first modeled by a state-averaged generalized-active-space self-consistent-field reference, followed by a treatment of dynamical electron correlation via the state-averaged MR-DSRG approach. The state-averaged formalism is essential for modeling the high density of core-excited states in large organic systems and helps avoid root-flipping issues that arise in state-specific methods. Several approximations to the full valence active space were considered to truncate the determinant space of the largest molecules in the XABOOM set. The effect of the two approximations that split the orbital space and restrict the valence space to only the π orbitals are tested on the core-excited states of N_2O and O_3. Both approximations affect the energy splittings by less than 0.3 eV in N_2O. Still, these approximations can lead to large energy errors in the case of O_3 since the partitioning of the determinant space is inconsistent with the strong coupling between core-excited states observed in the full valence space. We also investigated the choice of the flow parameter s, finding that $s = 1\ E_\mathrm{h}^{-2}$ is an appropriate value for GAS-DSRG calculations on organic systems.

We report the $1s \rightarrow \pi^*$ vertical transition energies and oscillator strengths of 40 molecules from second- and third-order DSRG treatments (DSRG-MRPT2/3) and find that these values are in good agreement with EOM-CCSD results.[80] Compared to existing experimental data, DSRG-MRPT3 transition energies agree better with absolute transition energies. At the same time, DSRG-MRPT2 and EOM-CCSD under and overestimate the transitions energies, showing a mean signed deviation of -0.74 and $+0.69$ eV, respectively. We also carefully analyzed ozone and glyoxylic acid, two molecules for which theoretical predictions show significant deviations. Besides its higher accuracy, the third-order GAS-DSRG approach shows several other advantages compared to DSRG-MRPT2 in computations of core-excited states. DSRG-MRPT3 is more likely to avoid any inconsistency in the order of eigenstates before and after the relaxation step, and it is less sensitive to intruders in systems like glyoxylic acid.

The present work also highlights some remaining challenges in describing core-excited methods with multireference methods. Firstly, limits on the size of the active space that can be treated with the GAS approach may affect the accuracy of computations on molecules larger than those in the XABOOM set. However, this restriction may also be relevant to special cases, like ozone, where

Accepted to J. Chem. Phys. 10.1063/5.0137096

ACCEPTED MANUSCRIPT

The Journal of Chemical Physics

This is the author's peer reviewed, accepted manuscript. However, the online version of record will be different from this version once it has been copyedited and typeset.
PLEASE CITE THIS ARTICLE AS DOI: 10.1063/5.0137096

AIP Publishing

a GAS larger than the full-valence space applied in this work may be necessary to reconcile the remaining differences between the experimental and theoretical spectra. Other challenges that should be targeted in future research include simplifying the selection of GAS orbitals, improving algorithms for the optimization of GASSCF reference states, and extending the formalism to improve the estimation of oscillator strengths. Lastly, we note that the approach pursued in this work obtains core excitation energies from separate computations on the ground and core-excited states. As such, one of its strengths is that it can accurately describe core-excited states, while one of its weaknesses is that it works best to describe a small number of states.[78] In contrast, methods that start from a correlated ground state and directly target the energy differences—including time-dependent DFT, EOM methods, and Green's function approaches—can directly target a large number of states in one computation and are formally more appealing. Therefore, a desirable extension of the present work would be to formulate a direct approach to target core excited states. Examples of multireference formalisms that explore this direction can be found in Refs. 70,75–77,135.

Despite these challenges, the GAS-DSRG method is well suited for the simulation of X-ray spectra of transient species, including applications to XTAS of molecules during chemical reactions. Further theoretical extensions of the approach to account for valence-excited states and their coupling to core-excited states would also allow simulating pump-probe UV/X-ray experiments to track electron and nuclear dynamics in photochemical processes. Other interesting future directions include the application of the GAS-DSRG method to the simulation of X-ray photoelectron spectroscopy and resonant-inelastic X-ray scattering.

SUPPLEMENTARY MATERIAL

See the supplementary material for: 1) active spaces and number of states used for GAS-DSRG approach of each molecule, 2) energy splittings and oscillator strength ratios for molecules with two or more transitions from the same element, 3) energies and oscillator strengths for 1,2-benzoquinone computed with different flow parameter values, and 4) GAS-DSRG transition energies, available experimental transition energies, and oscillator strengths of all molecules (xaboom_dsrg_data.xlsx).

Accepted to J. Chem. Phys. 10.1063/5.0137096

ACCEPTED MANUSCRIPT

The Journal of Chemical Physics

AIP Publishing

This is the author's peer reviewed, accepted manuscript. However, the online version of record will be different from this version once it has been copyedited and typeset.
PLEASE CITE THIS ARTICLE AS DOI: 10.1063/5.0137096

ACKNOWLEDGMENTS

The authors would like to thank Alexander Paul and Henrik Koch for providing the EOM-CC3 ozone results reported in this paper. This research was supported by the U.S. National Science Foundation under award number CHEM-1900532.

DATA AVAILABILITY

The data that supports the findings of this study are available within the article and its supplementary material.

REFERENCES

[1]F. De Groot, "High-resolution X-ray emission and X-ray absorption spectroscopy," Chem. Rev. **101**, 1779–1808 (2001).

[2]J. Yano and V. K. Yachandra, "X-ray absorption spectroscopy," Photosynth. Res. **102**, 241–254 (2009).

[3]G. Capano, C. J. Milne, M. Chergui, U. Rothlisberger, I. Tavernelli, and T. J. Penfold, "Probing wavepacket dynamics using ultrafast x-ray spectroscopy," J. Phys. B: At., Mol. Opt. Phys. **48** (2015).

[4]C. Li and F. A. Evangelista, "Driven similarity renormalization group: Third-order multireference perturbation theory," J. Chem. Phys. **146** (2017), 1701.02011.

[5]L. Barreau, A. D. Ross, S. Garg, P. M. Kraus, D. M. Neumark, and S. R. Leone, "Efficient table-top dual-wavelength beamline for ultrafast transient absorption spectroscopy in the soft X-ray region," Sci. Rep. **10**, 1–9 (2020).

[6]Y. Pertot, C. Schmidt, M. Matthews, A. Chauvet, M. Huppert, V. Svoboda, A. Von Conta, A. Tehlar, D. Baykusheva, J. P. Wolf, and H. J. Wörner, "Time-resolved x-ray absorption spectroscopy with a water window high-harmonic source," Science **355**, 264–267 (2017).

[7]A. D. Ross, D. Hait, V. Scutelnic, E. A. Haugen, E. Ridente, M. B. Balkew, D. M. Neumark, M. Head-Gordon, and S. R. Leone, "Jahn-Teller distortion and dissociation of CCl 4 + by transient X-ray spectroscopy simultaneously at the carbon K- and chlorine L-edge," Chem. Sci. **13**, 9310–9320 (2022).

[8]A. R. Attar, A. Bhattacherjee, C. D. Pemmaraju, K. Schnorr, K. D. Closser, D. Prendergast, and S. R. Leone, "Femtosecond x-ray spectroscopy of an electrocyclic ring-opening reaction,"

Accepted to J. Chem. Phys. 10.1063/5.0137096

ACCEPTED MANUSCRIPT

The Journal of Chemical Physics

AIP Publishing

This is the author's peer reviewed, accepted manuscript. However, the online version of record will be different from this version once it has been copyedited and typeset.
PLEASE CITE THIS ARTICLE AS DOI: 10.1063/5.0137096

Science **356**, 54–59 (2017).

[9]A. Bhattacherjee and S. R. Leone, "Ultrafast X-ray Transient Absorption Spectroscopy of Gas-Phase Photochemical Reactions: A New Universal Probe of Photoinduced Molecular Dynamics," Acc. Chem. Res. **51**, 3203–3211 (2018).

[10]R. Faber and S. Coriani, "Resonant Inelastic X-ray Scattering and Nonesonant X-ray Emission Spectra from Coupled-Cluster (Damped) Response Theory," J. Chem. Theory Comput. **15**, 520–528 (2019).

[11]V. Scutelnic, S. Tsuru, M. Pápai, Z. Yang, M. Epshtein, T. Xue, E. Haugen, Y. Kobayashi, A. I. Krylov, K. B. Møller, S. Coriani, and S. R. Leone, "X-ray transient absorption reveals the 1Au ($n\pi^*$) state of pyrazine in electronic relaxation," Nat. Commun. **12**, 6–13 (2021).

[12]M. L. Vidal, M. Epshtein, V. Scutelnic, Z. Yang, T. Xue, S. R. Leone, A. I. Krylov, and S. Coriani, "Interplay of Open-Shell Spin-Coupling and Jahn-Teller Distortion in Benzene Radical Cation Probed by X-ray Spectroscopy," J. Phys. Chem. A **124**, 9532–9541 (2020).

[13]M. Epshtein, V. Scutelnic, Z. Yang, T. Xue, M. L. Vidal, A. I. Krylov, S. Coriani, and S. R. Leone, "Table-Top X-ray Spectroscopy of Benzene Radical Cation," J. Phys. Chem. A **124**, 9524–9531 (2020).

[14]K. S. Zinchenko, F. Ardana-Lamas, I. Seidu, S. P. Neville, J. van der Veen, V. U. Lanfaloni, M. S. Schuurman, and H. J. Wörner, "Sub-7-femtosecond conical-intersection dynamics probed at the carbon K-edge," Science **371**, 489–494 (2021).

[15]P. Norman and A. Dreuw, "Simulating X-ray Spectroscopies and Calculating Core-Excited States of Molecules," Chem. Rev. **118**, 7208–7248 (2018).

[16]C. D. Rankine and T. J. Penfold, "Progress in the Theory of X-ray Spectroscopy: From Quantum Chemistry to Machine Learning and Ultrafast Dynamics," J. Phys. Chem. A **125**, 4276–4293 (2021).

[17]A. Schmitt and J. Schirmer, "Molecular K-shell excitation spectra in the relaxed-core Hartree-Fock approximation," Chem. Phys. **164**, 1–9 (1992).

[18]A. T. Gilbert, N. A. Besley, and P. M. Gill, "Self-consistent field calculations of excited states using the maximum overlap method (MOM)," J. Phys. Chem. A **112**, 13164–13171 (2008).

[19]N. A. Besley, A. T. B. Gilbert, and P. M. W. Gill, "Self-consistent-field calculations of core excited states," J. Chem. Phys. **130**, 124308 (2009).

[20]W. D. Derricotte and F. A. Evangelista, "Simulation of X-ray absorption spectra with orthogonality constrained density functional theory," Phys. Chem. Chem. Phys. **17**, 14360–14374

Accepted to J. Chem. Phys. 10.1063/5.0137096

ACCEPTED MANUSCRIPT

The Journal of Chemical Physics

AIP Publishing

This is the author's peer reviewed, accepted manuscript. However, the online version of record will be different from this version once it has been copyedited and typeset.
PLEASE CITE THIS ARTICLE AS DOI: 10.1063/5.0137096

(2015).

[21]D. Hait, E. A. Haugen, Z. Yang, K. J. Oosterbaan, S. R. Leone, and M. Head-Gordon, "Accurate prediction of core-level spectra of radicals at density functional theory cost via square gradient minimization and recoupling of mixed configurations," J. Chem. Phys. **153**, 134108 (2020), 2006.10181.

[22]D. Hait and M. Head-Gordon, "Highly Accurate Prediction of Core Spectra of Molecules at Density Functional Theory Cost: Attaining Sub-electronvolt Error from a Restricted Open-Shell Kohn-Sham Approach," J. Phys. Chem. Lett. **11**, 775–786 (2020), 1912.05249.

[23]M. Stener, G. Fronzoni, and M. de Simone, "Time dependent density functional theory of core electrons excitations," Chem. Phys. Lett. **373**, 115–123 (2003).

[24]A. Nakata, Y. Imamura, and H. Nakai, "Extension of the core-valence-Rydberg B3LYP functional to core-excited-state calculations of third-row atoms," J. Chem. Theory Comput. **3**, 1295–1305 (2007).

[25]U. Ekström, P. Norman, V. Carravetta, and H. Ågren, "Polarization propagator for X-ray spectra," Phys. Rev. Lett. **97**, 2–5 (2006).

[26]J.-W. Song, M. A. Watson, A. Nakata, and K. Hirao, "Core-excitation energy calculations with a long-range corrected hybrid exchange-correlation functional including a short-range Gaussian attenuation (LCgau-BOP)," J. Chem. Phys. **129**, 184113 (2008).

[27]N. A. Besley, M. J. Peach, and D. J. Tozer, "Time-dependent density functional theory calculations of near-edge X-ray absorption fine structure with short-range corrected functionals," Phys. Chem. Chem. Phys. **11**, 10350–10358 (2009).

[28]N. A. Besley, "Fast Time-Dependent Density Functional Theory Calculations of the X-ray Absorption Spectroscopy of Large Systems," J. Chem. Theory Comput. **12**, 5018–5025 (2016).

[29]W. Liang, S. A. Fischer, M. J. Frisch, and X. Li, "Energy-specific linear response TDHF/TDDFT for calculating high-energy excited states," J. Chem. Theory Comput. **7**, 3540–3547 (2011).

[30]Y. Zhang, J. D. Biggs, D. Healion, N. Govind, and S. Mukamel, "Core and valence excitations in resonant X-ray spectroscopy using restricted excitation window time-dependent density functional theory," J. Chem. Phys. **137**, 194306 (2012).

[31]P. J. Lestrange, P. D. Nguyen, and X. Li, "Calibration of Energy-Specific TDDFT for Modeling K-edge XAS Spectra of Light Elements," J. Chem. Theory Comput. **11**, 2994–2999 (2015).

[32]L. Triguero, L. Pettersson, and H. Ågren, "Calculations of near-edge x-ray-absorption spectra of gas-phase and chemisorbed molecules by means of density-functional and transition-potential

Accepted to J. Chem. Phys. 10.1063/5.0137096

ACCEPTED MANUSCRIPT

The Journal of Chemical Physics

AIP Publishing

This is the author's peer reviewed, accepted manuscript. However, the online version of record will be different from this version once it has been copyedited and typeset.
PLEASE CITE THIS ARTICLE AS DOI: 10.1063/5.0137096

theory," Phys. Rev. B: Condens. Matter Mater. Phys. **58**, 8097–8110 (1998).

[33]M. Leetmaa, M. P. Ljungberg, A. Lyubartsev, A. Nilsson, and L. G. Pettersson, "Theoretical approximations to X-ray absorption spectroscopy of liquid water and ice," J. Electron Spectrosc. Relat. Phenom. **177**, 135–157 (2010).

[34]P. Verma and R. J. Bartlett, "Increasing the applicability of density functional theory. V. X-ray absorption spectra with ionization potential corrected exchange and correlation potentials," J. Chem. Phys. **145** (2016), 10.1063/1.4955194.

[35]Y. Jin and R. J. Bartlett, "Accurate computation of X-ray absorption spectra with ionization potential optimized global hybrid functional," J. Chem. Phys. **149**, 064111 (2018).

[36]Y. C. Park, A. Perera, and R. J. Bartlett, "Density functionals for core excitations," J. Chem. Phys. **157**, 094107 (2022).

[37]F. A. Asmuruf and N. A. Besley, "Calculation of near-edge X-ray absorption fine structure with the CIS(D) method," Chem. Phys. Lett. **463**, 267–271 (2008).

[38]M. Roemelt, D. Maganas, S. DeBeer, and F. Neese, "A combined DFT and restricted open-shell configuration interaction method including spin-orbit coupling: Application to transition metal L-edge X-ray absorption spectroscopy," J. Chem. Phys. **138**, 204101 (2013).

[39]D. Maganas, M. Roemelt, M. Hävecker, A. Trunschke, A. Knop-Gericke, R. Schlögl, and F. Neese, "First principles calculations of the structure and V L-edge X-ray absorption spectra of V_2O_5 using local pair natural orbital coupled cluster theory and spin–orbit coupled configuration interaction approaches," Phys. Chem. Chem. Phys. **15**, 7260 (2013).

[40]D. Maganas, S. Debeer, and F. Neese, "Pair Natural Orbital Restricted Open-Shell Configuration Interaction (PNO-ROCIS) Approach for Calculating X-ray Absorption Spectra of Large Chemical Systems," J. Phys. Chem. A **122**, 1215–1227 (2018).

[41]K. J. Oosterbaan, A. F. White, and M. Head-Gordon, "Non-orthogonal configuration interaction with single substitutions for the calculation of core-excited states," J. Chem. Phys. **149**, 044116 (2018).

[42]K. J. Oosterbaan, A. F. White, and M. Head-Gordon, "Non-Orthogonal Configuration Interaction with Single Substitutions for Core-Excited States: An Extension to Doublet Radicals," J. Chem. Theory Comput. **15**, 2966–2973 (2019).

[43]S. M. Garner and E. Neuscamman, "Core excitations with excited state mean field and perturbation theory," J. Chem. Phys. **153**, 154102 (2020).

Accepted to J. Chem. Phys. 10.1063/5.0137096

ACCEPTED MANUSCRIPT

The Journal of Chemical Physics

AIP Publishing

This is the author's peer reviewed, accepted manuscript. However, the online version of record will be different from this version once it has been copyedited and typeset.
PLEASE CITE THIS ARTICLE AS DOI: 10.1063/5.0137096

[44]S. Coriani, O. Christiansen, T. Fransson, and P. Norman, "Coupled-cluster response theory for near-edge x-ray-absorption fine structure of atoms and molecules," Phys. Rev. A: At., Mol., Opt. Phys. **85**, 1–8 (2012).

[45]S. Coriani, T. Fransson, O. Christiansen, and P. Norman, "Asymmetric-lanczos-chain-driven implementation of electronic resonance convergent coupled-cluster linear response theory," J. Chem. Theory Comput. **8**, 1616–1628 (2012).

[46]S. Coriani and H. Koch, "Communication: X-ray absorption spectra and core-ionization potentials within a core-valence separated coupled cluster framework," J. Chem. Phys. **143**, 181103 (2015).

[47]R. Faber and S. Coriani, "Core-valence-separated coupled-cluster-singles-and-doubles complex-polarization-propagator approach to X-ray spectroscopies," Phys. Chem. Chem. Phys. **22**, 2642–2647 (2020).

[48]M. Nooijen and R. J. Bartlett, "Description of core-excitation spectra by the open-shell electron-attachment equation-of-motion coupled cluster method," J. Chem. Phys. **102**, 6735–6756 (1995).

[49]B. Peng, P. J. Lestrange, J. J. Goings, M. Caricato, and X. Li, "Energy-Specific Equation-of-Motion Coupled-Cluster Methods for High-Energy Excited States: Application to K-edge X-ray Absorption Spectroscopy," J. Chem. Theory Comput. **11**, 4146–4153 (2015).

[50]A. P. Bazante, A. Perera, and R. J. Bartlett, "Towards core-excitation spectra in attosecond spectroscopy: A coupled-cluster study of ClF," Chem. Phys. Lett. **683**, 68–75 (2017).

[51]M. L. Vidal, X. Feng, E. Epifanovsky, A. I. Krylov, and S. Coriani, "New and Efficient Equation-of-Motion Coupled-Cluster Framework for Core-Excited and Core-Ionized States," J. Chem. Theory Comput. **15**, 3117–3133 (2019).

[52]M. L. Vidal, A. I. Krylov, and S. Coriani, "Dyson orbitals within the fc-CVS-EOM-CCSD framework: theory and application to X-ray photoelectron spectroscopy of ground and excited states," Phys. Chem. Chem. Phys. **22**, 2693–2703 (2020).

[53]K. D. Nanda and A. I. Krylov, "Cherry-picking resolvents: A general strategy for convergent coupled-cluster damped response calculations of core-level spectra," J. Chem. Phys. **153**, 141104 (2020).

[54]S. D. Folkestad and H. Koch, "Equation-of-Motion MLCCSD and CCSD-in-HF Oscillator Strengths and Their Application to Core Excitations," J. Chem. Theory Comput. **16**, 6869–6879 (2020).

Accepted to J. Chem. Phys. 10.1063/5.0137096

ACCEPTED MANUSCRIPT

The Journal of Chemical Physics

AIP Publishing

This is the author's peer reviewed, accepted manuscript. However, the online version of record will be different from this version once it has been copyedited and typeset.
PLEASE CITE THIS ARTICLE AS DOI: 10.1063/5.0137096

[55]R. H. Myhre, S. Coriani, and H. Koch, "Near-Edge X-ray Absorption Fine Structure within Multilevel Coupled Cluster Theory," J. Chem. Theory Comput. **12**, 2633–2643 (2016).

[56]Y. C. Park, A. Perera, and R. J. Bartlett, "Equation of motion coupled-cluster for core excitation spectra: Two complementary approaches," J. Chem. Phys. **151**, 164117 (2019).

[57]R. Peng, A. V. Copan, and A. Y. Sokolov, "Simulating X-ray Absorption Spectra with Linear-Response Density Cumulant Theory," J. Phys. Chem. A **123**, 1840–1850 (2019).

[58]J. Wenzel, M. Wormit, and A. Dreuw, "Calculating X-ray absorption spectra of open-shell molecules with the unrestricted algebraic-diagrammatic construction scheme for the polarization propagator," J. Chem. Theory Comput. **10**, 4583–4598 (2014).

[59]J. Wenzel, M. Wormit, and A. Dreuw, "Calculating core-level excitations and x-ray absorption spectra of medium-sized closed-shell molecules with the algebraic-diagrammatic construction scheme for the polarization propagator," J. Comput. Chem. **35**, 1900–1915 (2014).

[60]J. Wenzel, A. Holzer, M. Wormit, and A. Dreuw, "Analysis and comparison of CVS-ADC approaches up to third order for the calculation of core-excited states," J. Chem. Phys. **142**, 214104 (2015).

[61]D. A. Matthews, "EOM-CC methods with approximate triple excitations applied to core excitation and ionisation energies," Mol. Phys. **118**, e1771448 (2020).

[62]J. E. Arias-Martinez, L. A. Cunha, K. J. Oosterbaan, J. Lee, and M. Head-Gordon, "Accurate core excitation and ionization energies from a state-specific coupled-cluster singles and doubles approach," Phys. Chem. Chem. Phys. **24**, 20728–20741 (2022).

[63]M. Simons and D. A. Matthews, "Transition-potential coupled cluster," J. Chem. Phys. **154**, 014106 (2021).

[64]Y. C. Park, A. Perera, and R. J. Bartlett, "Equation of motion coupled-cluster study of core excitation spectra II: Beyond the dipole approximation," J. Chem. Phys. **155** (2021), 10.1063/5.0059276.

[65]A. C. Paul, R. H. Myhre, and H. Koch, "New and Efficient Implementation of CC3," J. Chem. Theory Comput. **17**, 117–126 (2021), arXiv:2007.01088.

[66]A. B. Rocha, "Potential curves for inner-shell states of CO calculated at multiconfigurational self-consistent field level," J. Chem. Phys. **134**, 024107 (2011).

[67]M. Alagia, E. Bodo, P. Decleva, S. Falcinelli, A. Ponzi, R. Richter, and S. Stranges, "The soft X-ray absorption spectrum of the allyl free radical," Phys. Chem. Chem. Phys. **15**, 1310–1318 (2013).

Accepted to J. Chem. Phys. 10.1063/5.0137096

ACCEPTED MANUSCRIPT

The Journal of Chemical Physics

AIP Publishing

This is the author's peer reviewed, accepted manuscript. However, the online version of record will be different from this version once it has been copyedited and typeset.
PLEASE CITE THIS ARTICLE AS DOI: 10.1063/5.0137096

[68]M. Guo, L. K. Sørensen, M. G. Delcey, R. V. Pinjari, and M. Lundberg, "Simulations of iron K pre-edge X-ray absorption spectra using the restricted active space method," Phys. Chem. Chem. Phys. **18**, 3250–3259 (2016).

[69]B. Helmich-Paris, "Simulating X-ray absorption spectra with complete active space self-consistent field linear response methods," Int. J. Quantum Chem. **121**, 1–20 (2021).

[70]C. E. V. de Moura and A. Y. Sokolov, "Simulating X-ray photoelectron spectra with strong electron correlation using multireference algebraic diagrammatic construction theory," Phys. Chem. Chem. Phys. **24**, 4769–4784 (2022).

[71]W. Butscher, R. J. Buenker, and S. D. Peyerimhoff, "All-electron CI calculations for core-ionized, core-valence excited and shake-up states of N_2," Chem. Phys. Lett. **52**, 449–456 (1977).

[72]J. P. Coe and M. J. Paterson, "Multireference X-ray emission and absorption spectroscopy calculations from Monte Carlo configuration interaction," Theor. Chem. Acc. **134**, 3–9 (2015).

[73]A. Lisini and P. Decleva, "Calculation of dynamical correlation effects by quasidegenerate perturbation theory. An application to photoionization spectra," Chem. Phys. **168**, 1–13 (1992).

[74]J. Brabec, K. Bhaskaran-Nair, N. Govind, J. Pittner, and K. Kowalski, "Communication: Application of state-specific multireference coupled cluster methods to core-level excitations," J. Chem. Phys. **137**, 1–5 (2012).

[75]S. Sen, A. Shee, and D. Mukherjee, "A study of the ionisation and excitation energies of core electrons using a unitary group adapted state universal approach," Mol. Phys. **111**, 2625–2639 (2013).

[76]A. K. Dutta, J. Gupta, N. Vaval, and S. Pal, "Intermediate Hamiltonian Fock space multireference coupled cluster approach to core excitation spectra," J. Chem. Theory Comput. **10**, 3656–3668 (2014).

[77]D. Maganas, J. K. Kowalska, M. Nooijen, S. DeBeer, and F. Neese, "Comparison of multireference ab initio wavefunction methodologies for X-ray absorption edges: A case study on [Fe(II/III)Cl 4] 2–/1– molecules," J. Chem. Phys. **150**, 104106 (2019).

[78]M. Huang, C. Li, and F. A. Evangelista, "Theoretical Calculation of Core-Excited States along Dissociative Pathways beyond Second-Order Perturbation Theory," J. Chem. Theory Comput. **18**, 219–233 (2022).

[79]C. Li and F. A. Evangelista, "Driven similarity renormalization group for excited states: A state-averaged perturbation theory," J. Chem. Phys. **148**, 124106 (2018).

Accepted to J. Chem. Phys. 10.1063/5.0137096

ACCEPTED MANUSCRIPT

The Journal of Chemical Physics

AIP Publishing

This is the author's peer reviewed, accepted manuscript. However, the online version of record will be different from this version once it has been copyedited and typeset.
PLEASE CITE THIS ARTICLE AS DOI: 10.1063/5.0137096

[80]T. Fransson, I. E. Brumboiu, M. L. Vidal, P. Norman, S. Coriani, and A. Dreuw, "XABOOM: An X-ray Absorption Benchmark of Organic Molecules Based on Carbon, Nitrogen, and Oxygen 1s $\rightarrow \pi^*$ Transitions," J. Chem. Theory Comput. **17**, 1618–1637 (2021).

[81]J. F. Stanton and R. J. Bartlett, "The equation of motion coupled-cluster method. A systematic biorthogonal approach to molecular excitation energies, transition probabilities, and excited state properties," J. Chem. Phys. **98**, 7029–7039 (1993).

[82]R. V. Pinjari, M. G. Delcey, M. Guo, M. Odelius, and M. Lundberg, "Restricted active space calculations of L-edge X-ray absorption spectra: From molecular orbitals to multiplet states," J. Chem. Phys. **141** (2014).

[83]R. C. Couto, L. Kjellsson, H. Ågren, V. Carravetta, S. L. Sorensen, M. Kubin, C. Bülow, M. Timm, V. Zamudio-Bayer, B. von Issendorff, J. T. Lau, J. Söderström, J.-E. Rubensson, and R. Lindblad, "The carbon and oxygen K-edge NEXAFS spectra of CO^+," Phys. Chem. Chem. Phys. **22**, 16215–16223 (2020).

[84]R. Lindblad, L. Kjellsson, R. C. Couto, M. Timm, C. Bülow, V. Zamudio-Bayer, M. Lundberg, B. Von Issendorff, J. T. Lau, S. L. Sorensen, V. Carravetta, H. Ågren, and J. E. Rubensson, "X-Ray Absorption Spectrum of the $N_2{}^+$ Molecular Ion," Phys. Rev. Lett. **124**, 203001 (2020).

[85]W. Kutzelnigg and D. Mukherjee, "Normal order and extended Wick theorem for a multiconfiguration reference wave function," J. Chem. Phys. **107**, 432–449 (1997).

[86]D. Mukherjee, "Normal ordering and a Wick-like reduction theorem for fermions with respect to a multi-determinantal reference state," Chem. Phys. Lett. **274**, 561–566 (1997).

[87]C. Li and F. A. Evangelista, "Multireference driven similarity renormalization group: A second-order perturbative analysis," J. Chem. Theory Comput. **11**, 2097–2108 (2015).

[88]C. Li and F. A. Evangelista, "Spin-free formulation of the multireference driven similarity renormalization group: A benchmark study of first-row diatomic molecules and spin-crossover energetics," J. Chem. Phys. **155**, 114111 (2021), 2106.07097.

[89]C. Li and F. A. Evangelista, "Towards numerically robust multireference theories: The driven similarity renormalization group truncated to one- and two-body operators," J. Chem. Phys. **144**, 164114 (2016).

[90]T. H. Dunning, "Gaussian basis sets for use in correlated molecular calculations. I. The atoms boron through neon and hydrogen," J. Chem. Phys. **90**, 1007–1023 (1989).

[91]F. Weigend, A. Köhn, and C. Hättig, "Efficient use of the correlation consistent basis sets in resolution of the identity MP2 calculations," J. Chem. Phys. **116**, 3175–3183 (2002).

Accepted to J. Chem. Phys. 10.1063/5.0137096

ACCEPTED MANUSCRIPT

The Journal of Chemical Physics

AIP Publishing

This is the author's peer reviewed, accepted manuscript. However, the online version of record will be different from this version once it has been copyedited and typeset.
PLEASE CITE THIS ARTICLE AS DOI: 10.1063/5.0137096

[92]F. Weigend, "A fully direct RI-HF algorithm: Implementation, optimised auxiliary basis sets, demonstration of accuracy and efficiency," Phys. Chem. Chem. Phys. **4**, 4285–4291 (2002).

[93]M. Wang, W.-H. Fang, and C. Li, "Assessment of State-Averaged Driven Similarity Renormalization Group on Vertical Excitation Energies: Optimal Flow Parameters and Applications to Nucleobases," J. Chem. Theory Comput. **19**, 122–136 (2023).

[94]A. Hitchcock and C. Brion, "Inner shell electron energy loss studies of HCN and C2N2," Chem. Phys. **37**, 319–331 (1979).

[95]S. J. Osborne, A. Ausmees, S. Svensson, A. Kivimäki, O. Sairanen, A. N. de Brito, H. Aksela, and S. Aksela, "The vibrationally resolved participator Auger spectra of selectively excited C 1s $(2\sigma)^{-1}$ $2\pi^1$ vibrational states in carbon monoxide," J. Chem. Phys. **102**, 7317–7324 (1995).

[96]R. Püttner, I. Dominguez, T. J. Morgan, C. Cisneros, R. F. Fink, E. Rotenberg, T. Warwick, M. Domke, G. Kaindl, and A. S. Schlachter, "Vibrationally resolved O 1s core-excitation spectra of CO and NO," Phys. Rev. A: At., Mol., Opt. Phys. **59**, 3415–3423 (1999).

[97]R. McLaren, S. A. Clark, I. Ishii, and A. P. Hitchcock, "Absolute oscillator strengths from K-shell electron-energy-loss spectra of the fluoroethenes and 1,3-perfluorobutadiene," Phys. Rev. A **36**, 1683–1701 (1987).

[98]G. Remmers, M. Domke, A. Puschmann, T. Mandel, C. Xue, G. Kaindl, E. Hudson, and D. A. Shirley, "High-resolution K-shell photoabsorption in formaldehyde," Phys. Rev. A **46**, 3935–3944 (1992).

[99]A. P. Hitchcock, M. Tronc, and A. Modelli, "Electron transmission and inner-shell electron energy loss spectroscopy of CH3CN, CH3NC, CH3SCN, and CH3NCS," J. Phys. Chem. **93**, 3068–3077 (1989).

[100]K. C. Prince, L. Avaldi, M. Coreno, R. Camilloni, and M. de Simone, "Vibrational structure of core to Rydberg state excitations of carbon dioxide and dinitrogen oxide," J. Phys. B: At., Mol. Opt. Phys. **32**, 2551–2567 (1999).

[101]L. Rosenqvist, K. Wiesner, A. Naves de Brito, M. Bässler, R. Feifel, I. Hjelte, C. Miron, H. Wang, M. N. Piancastelli, S. Svensson, O. Björneholm, and S. L. Sorensen, "Femtosecond dissociation of ozone studied by the Auger Doppler effect," J. Chem. Phys. **115**, 3614–3620 (2001).

[102]M. B. Robin, I. Ishii, R. McLaren, and A. P. Hitchcock, "Fluorination effects on the inner-shell spectra of unsaturated molecules," J. Electron Spectrosc. Relat. Phenom. **47**, 53–92 (1988).

[103]A. S. Vinogradov, V. N. Akimov, S. V. Nekipelov, A. A. Pavlychev, A. A. Boronoev, and A. V. Zhadenov, "X-ray absorption spectra of the nitromethane molecule CH3NO2," Opt. Spectrosc.

Accepted to J. Chem. Phys. 10.1063/5.0137096

ACCEPTED MANUSCRIPT

The Journal of Chemical Physics

AIP Publishing

This is the author's peer reviewed, accepted manuscript. However, the online version of record will be different from this version once it has been copyedited and typeset.
PLEASE CITE THIS ARTICLE AS DOI: 10.1063/5.0137096

72, 599–603 (1992).

[104]E. Rühl, A. T. Wen, and A. P. Hitchcock, "Inner-shell excitation of η5-C5H5Co(CO)2 and related compounds studied by gas phase electron energy loss spectroscopy," J. Electron Spectrosc. Relat. Phenom. **57**, 137–164 (1991).

[105]D. Duflot, J.-P. Flament, A. Giuliani, J. Heinesch, and M.-J. Hubin-Franskin, "Core shell excitation of furan at the O1s and C1s edges: An experimental and ab initio study," J. Chem. Phys. **119**, 8946–8955 (2003).

[106]E. Apen, A. P. Hitchcock, and J. L. Gland, "Experimental studies of the core excitation of imidazole, 4,5-dicyanoimidazole, and s-triazine," J. Phys. Chem. **97**, 6859–6866 (1993).

[107]C. Hennig, K. Hallmeier, A. Bach, S. Bender, R. Franke, J. Hormes, and R. Szargan, "Influence of substituents on the N K X-ray absorption near-edge structure of pyrrole derivatives," Spectrochim. Acta, Part A **52**, 1079–1083 (1996).

[108]G. Vall-Llosera, B. Gao, A. Kivimäki, M. Coreno, J. Álvarez Ruiz, M. De Simone, H. Ågren, and E. Rachlew, "The C 1s and N 1s near edge x-ray absorption fine structure spectra of five azabenzenes in the gas phase," J. Chem. Phys. **128** (2008).

[109]A. P. Hitchcock, Unpublished data, http://unicorn.mcmaster.ca/corex/cedb-title.html.

[110]A. P. Hitchcock and J. Stöhr, Unpublished data, http://unicorn.mcmaster.ca/corex/cedb-title.html.

[111]A. Hitchcock and D. Mancini, "Bibliography and database of inner shell excitation spectra of gas phase atoms and molecules," J. Electron Spectrosc. Relat. Phenom. **67**, 1–12 (1994).

[112]V. Feyer, O. Plekan, R. Richter, M. Coreno, M. De Simone, K. C. Prince, A. B. Trofimov, I. L. Zaytseva, and J. Schirmer, "Tautomerism in cytosine and uracil: A theoretical and experimental X-ray absorption and resonant auger study," J. Phys. Chem. A **114**, 10270–10276 (2010).

[113]J. T. Francis and A. P. Hitchcock, "Distinguishing keto and enol structures by inner-shell spectroscopy," J. Phys. Chem. **98**, 3650–3657 (1994).

[114]A. P. Hitchcock, P. Fischer, A. Gedanken, and M. B. Robin, "Antibonding σ^* valence MOs in the inner-shell and outer-shell spectra of the fluorobenzenes," J. Phys. Chem. **91**, 531–540 (1987).

[115]O. Plekan, V. Feyer, R. Richter, M. Coreno, M. de Simone, K. C. Prince, A. B. Trofimov, E. V. Gromov, I. L. Zaytseva, and J. Schirmer, "A theoretical and experimental study of the near edge X-ray absorption fine structure (NEXAFS) and X-ray photoelectron spectra (XPS) of nucleobases: Thymine and adenine," Chem. Phys. **347**, 360–375 (2008).

Accepted to J. Chem. Phys. 10.1063/5.0137096

ACCEPTED MANUSCRIPT

The Journal of Chemical Physics

AIP Publishing

This is the author's peer reviewed, accepted manuscript. However, the online version of record will be different from this version once it has been copyedited and typeset.
PLEASE CITE THIS ARTICLE AS DOI: 10.1063/5.0137096

[116]N. Schmidt, J. Wenzel, A. Dreuw, R. H. Fink, and W. Hieringer, "Matrix effects in the C 1s photoabsorption spectra of condensed naphthalene," J. Chem. Phys. **145**, 234307 (2016).

[117]Y. Zubavichus, A. Shaporenko, V. Korolkov, M. Grunze, and M. Zharnikov, "X-ray absorption spectroscopy of the nucleotide bases at the carbon, nitrogen, and oxygen K-edges," J. Phys. Chem. B **112**, 13711–13716 (2008).

[118]J. Sous, P. Goel, and M. Nooijen, "Similarity transformed equation of motion coupled cluster theory revisited: A benchmark study of valence excited states," Mol. Phys. **112**, 616–638 (2014).

[119]V. Rishi, A. Perera, M. Nooijen, and R. J. Bartlett, "Excited states from modified coupled cluster methods: Are they any better than EOM CCSD?" J. Chem. Phys. **146**, 144104 (2017).

[120]A. Paul and H. Koch, Private Communication.

[121]B. N. C. Tenorio, K. B. Møller, P. Decleva, and S. Coriani, "Disentangling the resonant Auger spectra of ozone: overlapping core-hole states and core-excited state dynamics," Phys. Chem. Chem. Phys. **24**, 28150–28163 (2022).

[122]R. A. Kendall, T. H. Dunning, and R. J. Harrison, "Electron affinities of the first-row atoms revisited. Systematic basis sets and wave functions," J. Chem. Phys. **96**, 6796–6806 (1992).

[123]S. Stranges, M. Alagia, G. Fronzoni, and P. Decleva, "High-Resolution Inner-Shell Photoabsorption and Dissociation of Ozone," J. Phys. Chem. A **105**, 3400–3406 (2001).

[124]E. F. Hayes and A. K. Q. Siu, "Electronic structure of the open forms of three-membered rings," J. Am. Chem. Soc. **93**, 2090–2091 (1971).

[125]P. J. Hay, T. H. Dunning, and W. A. Goddard, "Configuration interaction studies of O 3 and O + 3 . Ground and excited states," J. Chem. Phys. **62**, 3912–3924 (1975).

[126]W. D. Laidig and H. F. Schaefer, "Large multiconfiguration self-consistent-field wave functions for the ozone molecule," J. Chem. Phys. **74**, 3411–3414 (1981).

[127]M. W. Schmidt and M. S. Gordon, "The construction and interpretation of MCSCF wavefunctions," Annu. Rev. Phys. Chem. **49**, 233–266 (1998).

[128]A. Kalemos and A. Mavridis, "Electronic structure and bonding of ozone," J. Chem. Phys. **129**, 054312 (2008).

[129]M. Musiał, S. A. Kucharski, P. Zerzucha, T. Kuś, and R. J. Bartlett, "Excited and ionized states of the ozone molecule with full triples coupled cluster methods," J. Chem. Phys. **131**, 194104 (2009).

[130]G. A. Oyedepo and A. K. Wilson, "Multireference correlation consistent composite approach [MR-ccCA]: Toward accurate prediction of the energetics of excited and transition state chem-

Accepted to J. Chem. Phys. 10.1063/5.0137096

istry," J. Phys. Chem. A **114**, 8806–8816 (2010).

[131]K. Bhaskaran-Nair and K. Kowalski, "Note: Excited state studies of ozone using state-specific multireference coupled cluster methods," J. Chem. Phys. **137**, 2011–2013 (2012).

[132]E. Miliordos and S. S. Xantheas, "On the bonding nature of ozone (O3) and its sulfur-substituted analogues SO2, OS2, and S3: Correlation between their biradical character and molecular properties," J. Am. Chem. Soc. **136**, 2808–2817 (2014).

[133]T. Y. Takeshita, B. A. Lindquist, and T. H. Dunning, "Insights into the electronic structure of ozone and sulfur dioxide from generalized valence bond theory: Bonding in O3 and SO2," J. Phys. Chem. A **119**, 7683–7694 (2015).

[134]T. Gejo, K. Okada, and T. Ibuki, "Photoabsorption spectrum of ozone in the K-edge region," Chem. Phys. Lett. **277**, 497–501 (1997).

[135]P. K. Samanta, D. Mukherjee, M. Hanauer, and A. Köhn, "Excited states with internally contracted multireference coupled-cluster linear response theory," J. Chem. Phys. **140**, 134108 (2014).

ACCEPTED MANUSCRIPT

The Journal of Chemical Physics

AIP Publishing

This is the author's peer reviewed, accepted manuscript. However, the online version of record will be different from this version once it has been copyedited and typeset.

PLEASE CITE THIS ARTICLE AS DOI: 10.1063/5.0137096

Accepted to J. Chem. Phys. 10.1063/5.0137096

ACCEPTED MANUSCRIPT

The Journal of Chemical Physics

AIP Publishing

This is the author's peer reviewed, accepted manuscript. However, the online version of record will be different from this version once it has been copyedited and typeset.
PLEASE CITE THIS ARTICLE AS DOI: 10.1063/5.0137096

TABLE II. Dependence of the transition energies (E, in eV) and oscillator strengths (f) for ethene, benzene and naphthalene as a function of the flow parameter s. Results were computed with a GASSCF reference and different levels of theory [PT2 = DSRG-MRPT2, PT3 = DSRG-MRPT3] using the cc-pVQZ basis. The values in the parenthesis are the relative energy with respect to $s = 1$ values.

Molecule	s	E(PT2)	f(PT2)	E(PT3)	f(PT3)
Ethene	0.125	284.97 (+0.66)	0.0783	285.29 (+0.15)	0.0772
	0.25	284.65 (+0.34)	0.0793	285.12 (−0.02)	0.0771
	0.5	284.45 (+0.14)	0.0804	285.10 (−0.05)	0.0766
	1	284.31	0.0814	285.14	0.0757
	2	284.18 (−0.13)	0.0826	285.18 (+0.03)	0.0746
	4	284.05 (−0.26)	0.0835	285.18 (+0.03)	0.0734
Benzene	0.125	286.78 (+3.20)	0.2646	287.31 (+1.98)	0.2651
	0.25	285.43 (+1.85)	0.2613	286.39 (+1.05)	0.2632
	0.5	284.26 (+0.68)	0.2555	285.67 (+0.34)	0.2610
	1	283.58	0.2488	285.33	0.2592
	2	283.36 (−0.23)	0.2432	285.27 (−0.06)	0.2586
	4	283.30 (−0.28)	0.2384	285.31 (−0.02)	0.2581
Naphthalene	0.125	286.49(+3.56)	0.1507	286.99 (+2.25)	0.1521
		286.76 (+3.57)	0.1571	287.24 (+2.26)	0.1601
		287.40 (+3.36)	0.0856	287.94 (+2.24)	0.0859
	0.25	285.02 (+2.08)	0.1455	285.95 (+1.20)	0.1499
		285.29 (+2.10)	0.1466	286.19 (+1.21)	0.1547
		285.93 (+1.90)	0.0819	286.91 (+1.22)	0.0839
	0.5	283.72 (+0.78)	0.1369	285.14 (+0.40)	0.1468
		283.99 (+0.80)	0.1308	285.38 (+0.40)	0.1491
		284.69 (+0.66)	0.0760	286.11 (+0.41)	0.0817
	1	282.93	0.1276	284.75	0.1440
		283.19	0.1152	284.98	0.1458
		284.03	0.0680	285.70	0.0802
	2	282.65 (−0.29)	0.1216	284.67 (−0.08)	0.1427
		282.88 (−0.31)	0.1072	284.89 (−0.09)	0.1451
		283.88 (−0.15)	0.0705	285.58 (−0.11)	0.0797
	4	282.57 (−0.37)	0.1190	284.70 (−0.04)	0.1415
		282.81 (−0.39)	0.1072	284.91 (−0.07)	0.1441
		283.92 (−0.12)	0.0610	285.56 (−0.14)	0.0792

Accepted to J. Chem. Phys. 10.1063/5.0137096

ACCEPTED MANUSCRIPT

The Journal of Chemical Physics

AIP Publishing

This is the author's peer reviewed, accepted manuscript. However, the online version of record will be different from this version once it has been copyedited and typeset.
PLEASE CITE THIS ARTICLE AS DOI: 10.1063/5.0137096

TABLE III. Absolute transition energies error statistics (in eV, MAD = Mean absolute deviation, MSD = Mean Signed Deviation, STD = Standard deviation). We report both statistics for the GAS-DSRG with respect to EOM-CCSD and for all theoretical methods with respect to available experimental data. For each set we list the number of transitions (N_T). GAS-DSRG results were computed with a GASSCF reference and different levels of theory [PT2 = DSRG-MRPT2, PT3 = DSRG-MRPT3] using the cc-pVQZ basis. EOM-CCSD(CC) results are taken from Ref. 80.

Transitions	Set	N_T	MAD	MSD	STD
C K-edge	PT2−CC	72	1.32	−1.32	0.64
	PT3−CC	72	0.43	−0.39	0.34
	PT2−Exp.	57	0.78	−0.77	0.55
	PT3−Exp.	57	0.29	0.08	0.33
	CC−Exp.	57	0.54	0.52	0.31
N K-edge	PT2−CC	21	1.27	−1.22	0.83
	PT3−CC	21	0.79	−0.76	0.58
	PT2−Exp.	17	0.69	−0.61	0.69
	PT3−Exp.	17	0.37	−0.11	0.37
	CC−Exp.	17	0.75	0.75	0.75
O K-edge	PT2−CC	22	1.95	−1.95	0.61
	PT3−CC	22	1.29	−1.29	0.56
	PT2−Exp.	17	0.77	−0.77	0.52
	PT3−Exp.	17	0.38	−0.11	0.46
	CC−Exp.	17	1.20	1.20	0.30
All	PT2−CC	116	1.44	−1.43	0.71
	PT3−CC	116	0.66	−0.64	0.56
	PT2−Exp.	91	0.76	−0.74	0.58
	PT3−Exp.	91	0.32	0.01	0.39
	CC−Exp.	91	0.70	0.69	0.40

Accepted to J. Chem. Phys. 10.1063/5.0137096

ACCEPTED MANUSCRIPT

The Journal of Chemical Physics

AIP Publishing

This is the author's peer reviewed, accepted manuscript. However, the online version of record will be different from this version once it has been copyedited and typeset.
PLEASE CITE THIS ARTICLE AS DOI: 10.1063/5.0137096

TABLE IV. Relative transition energies error statistics (in eV, MAD = Mean absolute deviation, MSD = Mean Signed Deviation, STD = Standard deviation). We report both statistics for the GAS-DSRG with respect to EOM-CCSD and for all theoretical methods with respect to available experimental data. For each set we list the number of transitions (N_T). GAS-DSRG results were computed with a GASSCF reference and different levels of theory [PT2 = DSRG-MRPT2, PT3 = DSRG-MRPT3] using the cc-pVQZ basis. EOM-CCSD(CC) results are taken from Ref. 80.

Set	N_T	MAD	MSD	STD
PT3−PT2	47	0.13	-0.02	0.17
CC−PT2	47	0.21	-0.12	0.25
CC−PT3	47	0.16	-0.11	0.19
PT2−Exp	34	0.24	0.08	0.30
PT3−Exp	34	0.19	0.05	0.24
CC−Exp	34	0.19	-0.07	0.30

TABLE V. Largest electron configuration contributions to relaxed GAS wave function for the three bright core-excited states in ozone. All terms are expressed with respect to the dominant ground state closed-shell configuration. The relaxed GAS wave function is obtained using MR-LDSRG(2) theory with a GASSCF reference (averaging over 16 states) and the cc-pVQZ basis.

State	Term	Weight (%)	Term	Weight (%)	Term	Weight (%)
$2a_1 \rightarrow 2b_1(\pi^*)$	$(2a_1)^{-1}(2b_1)^1$	58.4	$(1b_2)^{-1}(1a_2)^{-1}(2b_1)^2$	22.8	$(2a_1)^{-1}(6a_1)^{-1}(2b_1)^1(7a_1)^1$	1.6
$1a_1 \rightarrow 2b_1(\pi^*)$	$(1a_1)^{-1}(2b_1)^1$	64.8	$(1a_1)^{-1}(1a_2)^{-1}(2b_1)^2$	15.8	$(1a_1)^{-1}(3b_2)^{-1}(2b_1)^1(5b_2)^1$	2.7
$1b_2 \rightarrow 7a_1(\sigma^*)$	$(1b_2)^{-1}(7a_1)^1$	54.5	$(2a_1)^{-1}(1a_2)^{-1}(2b_1)^1(7a_1)^1$	18.3	$(2a_1)^{-1}(1a_2)^{-1}(1b_1)^{-1}(2b_1)^2(7a_1)^1$	2.0

Accepted to J. Chem. Phys. 10.1063/5.0137096

ACCEPTED MANUSCRIPT

The Journal of Chemical Physics

AIP Publishing

This is the author's peer reviewed, accepted manuscript. However, the online version of record will be different from this version once it has been copyedited and typeset.
PLEASE CITE THIS ARTICLE AS DOI: 10.1063/5.0137096

TABLE VI. Energies (E, in eV) and oscillator strengths for glyoxylic acid carbon K-edge transitions. Energy differences (ΔE, in eV) and oscillator strength ratios (r_f) between two transitions are also listed. Results were computed with a GASSCF reference and different levels of theory [PT2 = DSRG-MRPT2, PT3 = DSRG-MRPT3] using the cc-pVQZ basis.

	$5a' \rightarrow 4a''$		$4a' \rightarrow 4a''$			
Method	E	f	E	f	ΔE	r_f
PT2 ($s = 1$)	284.44	0.0635	286.08	0.0327	1.63	0.51
PT2 ($s = 0.5$)	284.87	0.0686	286.78	0.0508	1.91	0.74
PT2, SC ($s = 1$)	285.06	0.0537	286.78	0.0324	1.72	0.60
PT2, SC ($s = 0.5$)	285.18	0.0572	287.02	0.0398	1.83	0.70
PT3 ($s = 1$)	285.92	0.0715	288.01	0.0679	2.10	0.95
PT3 ($s = 0.5$)	286.13	0.0723	288.27	0.0712	2.14	0.98
PT3, SC ($s = 1$)	285.61	0.0623	287.60	0.0521	1.99	0.84
PT3, SC ($s = 0.5$)	285.63	0.0627	287.65	0.0535	2.02	0.85

Accepted to J. Chem. Phys. 10.1063/5.0137096

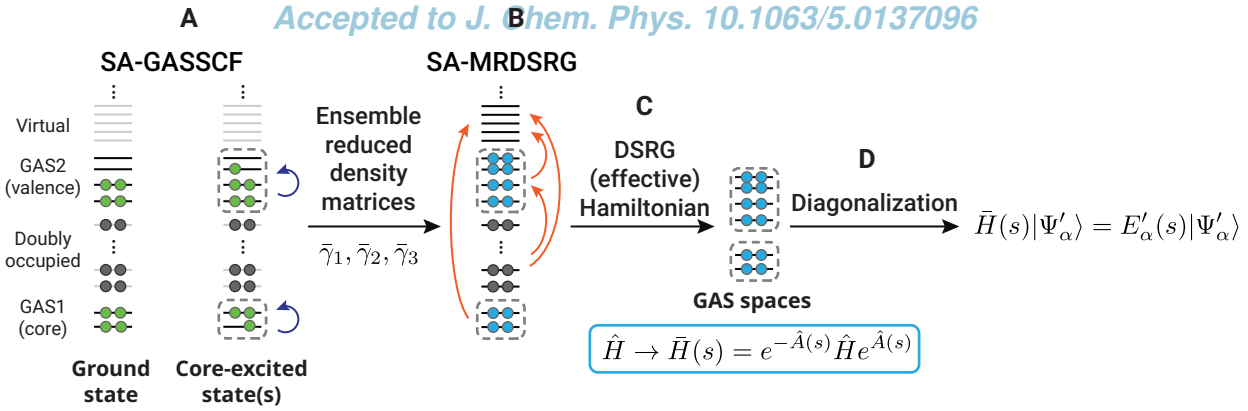

Acce J. Chem. Phys. 10.1063/5.0137096

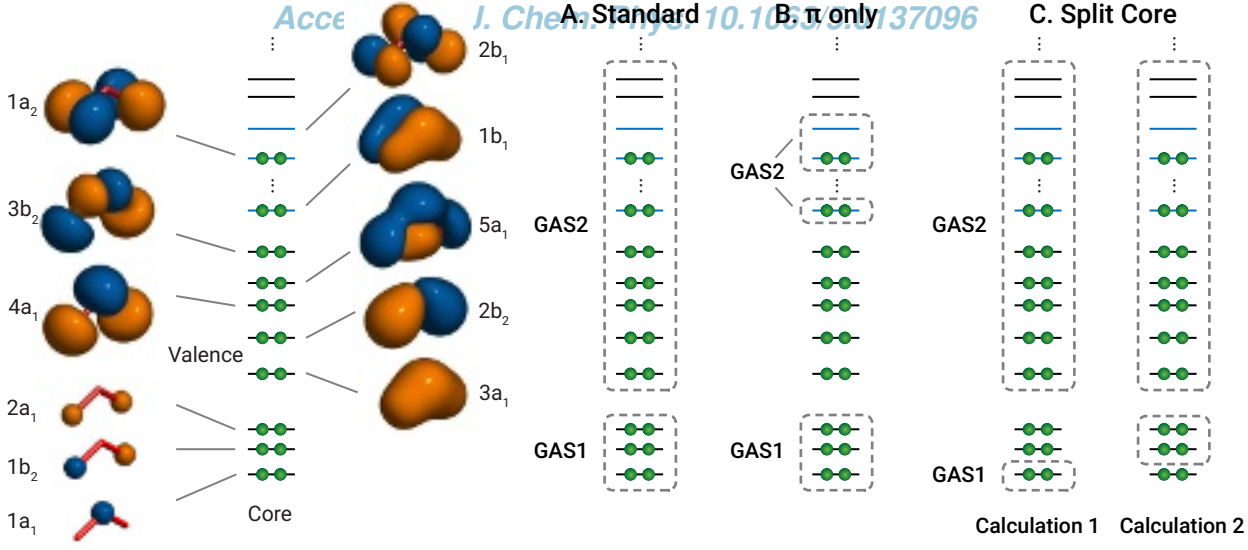

Accepted to J. Chem. Phys. 10.1063/5.0137096

A

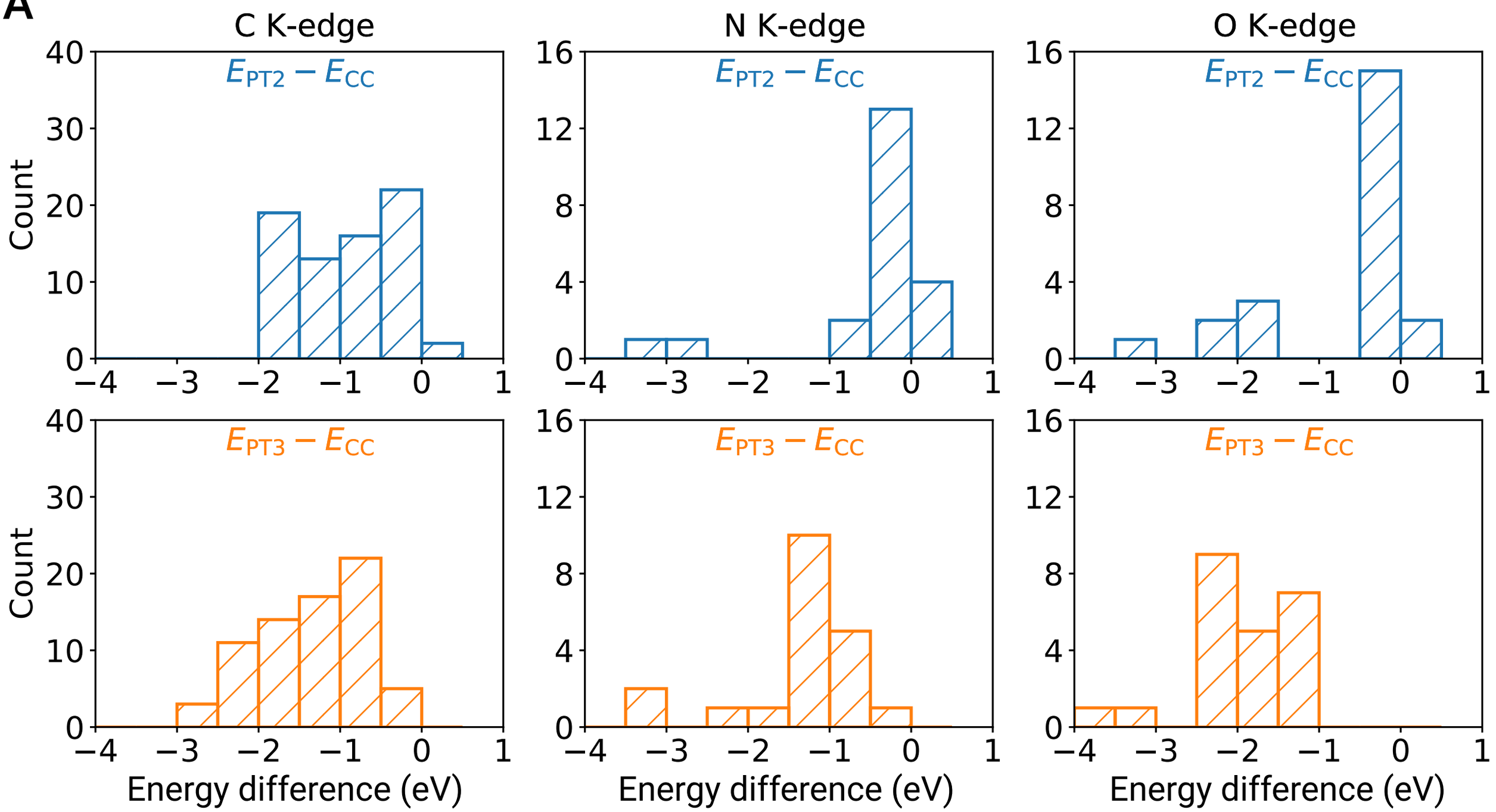

B

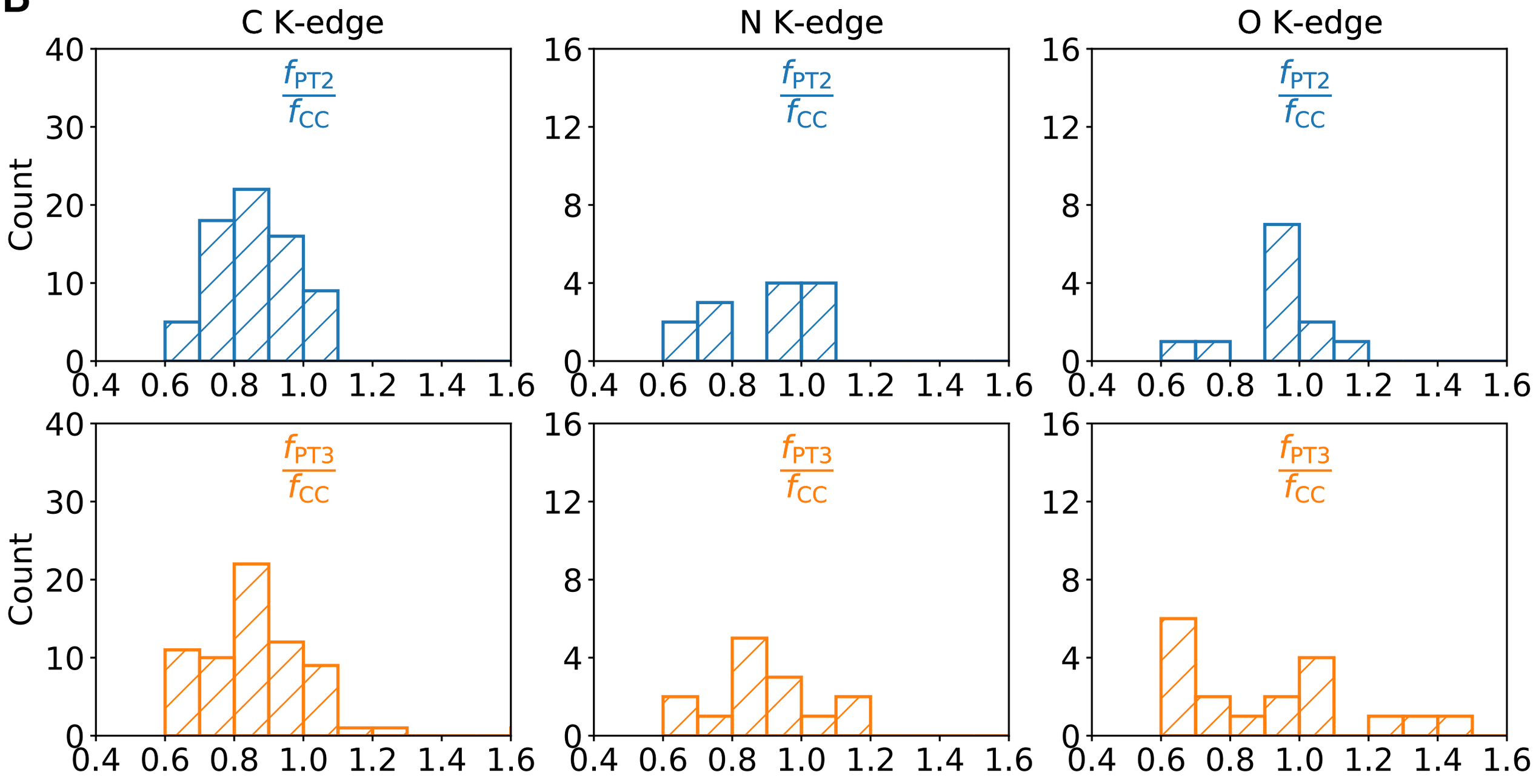

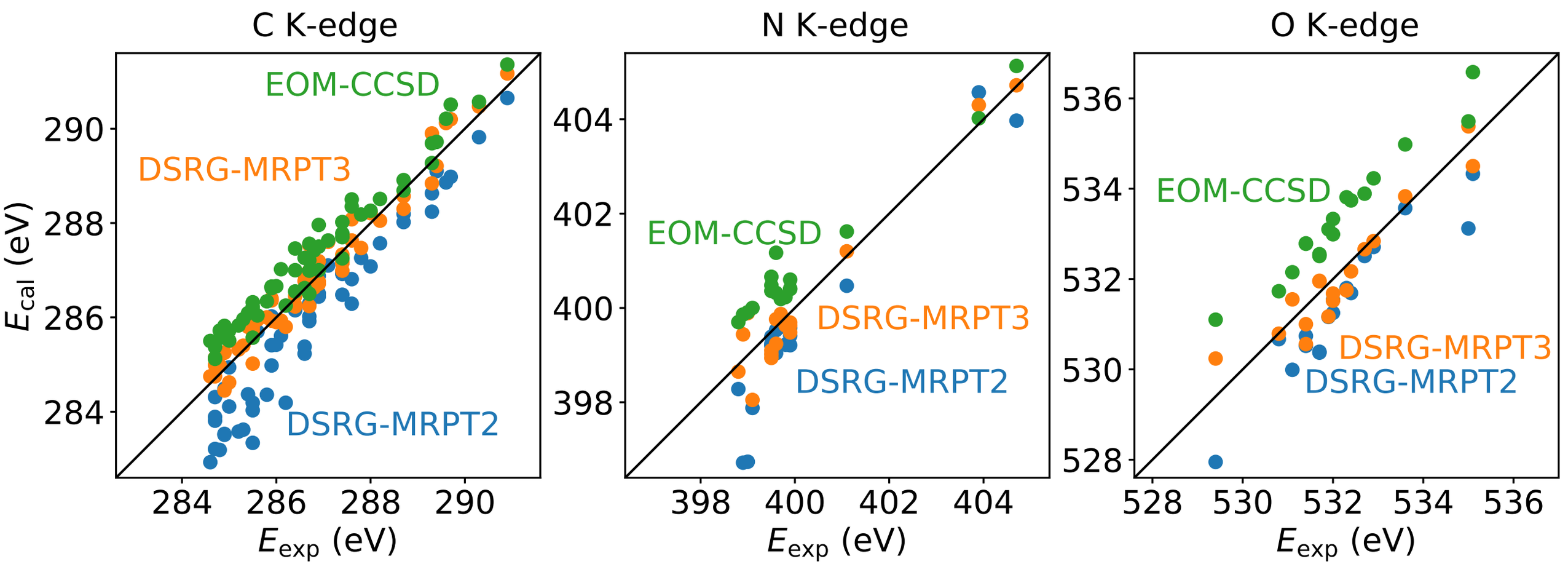
C K-edge
N K-edge
O K-edge
EOM-CCSD
DSRG-MRPT3
DSRG-MRPT2
E_{cal} (eV)
E_{exp} (eV)
284
286
288
290
398
400
402
404
528
530
532
534
536

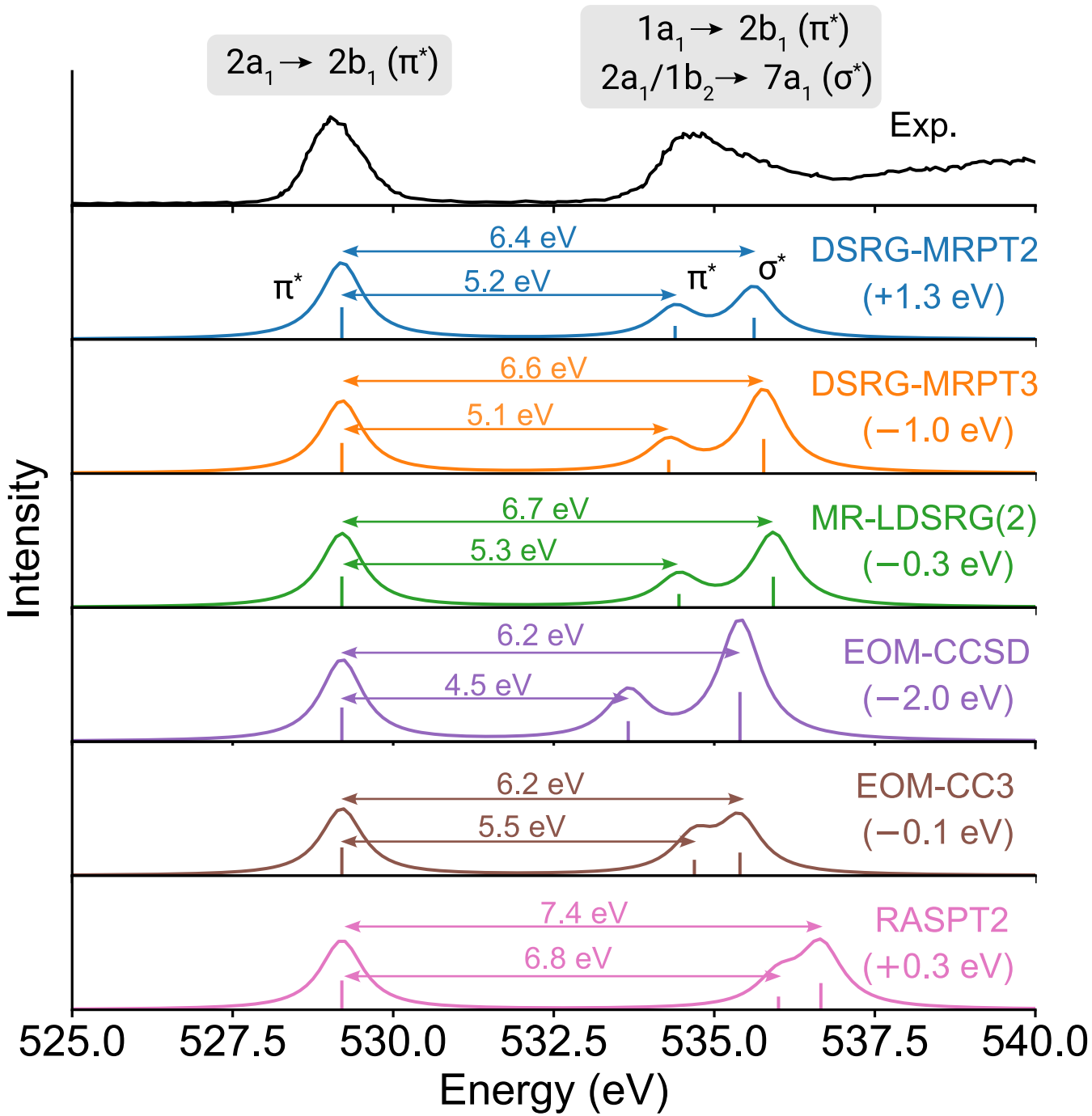
2a1 → 2b1 (π*)
1a1 → 2b1 (π*)
2a1/1b2 → 7a1 (σ*)
Exp.
6.4 eV
5.2 eV
π*
π*
σ*
DSRG-MRPT2
(+1.3 eV)
6.6 eV
5.1 eV
DSRG-MRPT3
(−1.0 eV)
6.7 eV
5.3 eV
MR-LDSRG(2)
(−0.3 eV)
6.2 eV
4.5 eV
EOM-CCSD
(−2.0 eV)
6.2 eV
5.5 eV
EOM-CC3
(−0.1 eV)
7.4 eV
6.8 eV
RASPT2
(+0.3 eV)
Intensity
525.0
527.5
530.0
532.5
535.0
537.5
540.0
Energy (eV)

Accepted to J. Chem. Phys.
10.1063/5.0137096